

## Original Article

**Cite this article:** Spry PG, Jansson NF, and Allen RL. A stable isotope (S, C and O) study of metamorphosed polymetallic sulphide deposits in the Bergslagen district, Sweden: The Stollberg example. *Geological Magazine* 161(e16): 1–16. <https://doi.org/10.1017/S0016756824000153>

Received: 17 February 2024

Revised: 15 May 2024

Accepted: 20 May 2024


**Keywords:**

stable isotopes; polymetallic sulphide deposits; Bergslagen district; Sweden; Stollberg deposit; metamorphosed

**Corresponding author:**

Paul G. Spry; Email: [pgspry@iastate.edu](mailto:pgspry@iastate.edu)

# A stable isotope (S, C and O) study of metamorphosed polymetallic sulphide deposits in the Bergslagen district, Sweden: The Stollberg example

Paul G. Spry<sup>1</sup> , Nils F. Jansson<sup>2</sup> and Rodney L. Allen<sup>3</sup>

<sup>1</sup>Department of the Earth, Atmosphere, and Climate, 253 Science Hall, Iowa State University, Ames, IA 50011-1027, USA; <sup>2</sup>Department of Civil, Environmental and Natural Resources Engineering, Luleå University, SE-971 87 Luleå, Sweden and <sup>3</sup>Volcanic Resources AB, Timotejvägen 18, 749 48 Enköping, Sweden

**Abstract**

The Paleoproterozoic Stollberg Zn-Pb-Ag plus magnetite ore field contains SVALS-type stratabound, limestone-skarn hosted sulphide deposits within volcanic (bimodal felsic and mafic rocks)/volcaniclastic rocks metamorphosed to the amphibolite facies. The sulphide ores consist of semi-massive to disseminated to vein-network sphalerite-galena and pyrrhotite (with subordinate pyrite, chalcopyrite, arsenopyrite and magnetite). Thermochemical considerations and stabilities of minerals in the systems K-Al-Si-O-H and Fe-S-O and sulphur isotope values for sulphides of  $\delta^{34}\text{S}_{\text{VCDT}} = +1.12$  to  $+5.71$  ‰ suggest that sulphur most likely formed by inorganic reduction of seawater sulphate that was carried in hydrothermally modified seawater fluid under the following approximate physicochemical conditions:  $T = 250^{\circ}\text{--}350^{\circ}\text{C}$ ,  $\delta^{34}\text{S}_{\text{SS}} = +3$  ‰,  $I = \sim 1$  m NaCl and a total dissolved S content of  $\sim 0.01$  to  $0.1$  moles/kg  $\text{H}_2\text{O}$ . However, a magmatic contribution of sulphur cannot be discounted. Carbon and oxygen isotope compositions of calcite in altered rocks spatially associated with mineralisation show values of  $\delta^{13}\text{C}_{\text{VPDB}} = -2.3$  to  $-0.8$  ‰ and  $\delta^{18}\text{O}_{\text{VSMOW}} = +9.5$  to  $+11.2$  ‰, with one anomalous sample exhibiting values of  $\delta^{13}\text{C}_{\text{VPDB}} = -0.1$  ‰ and  $\delta^{18}\text{O}_{\text{VSMOW}} = +10.9$  ‰. Most carbonates in ore show lighter C and O isotope values than those of Proterozoic (Orosirian) limestones and are likely the result of premetamorphic hydrothermal alteration involving modified seawater followed by decarbonation during regional metamorphism. The isotopically light C and O isotope values are consistent with those for carbonates spatially associated with other SVALS-type deposits in the Bergslagen ore district and suggest that such values may be used for exploration purposes.

**1. Introduction**

The Paleoproterozoic Bergslagen mining district, within the Bergslagen lithotectonic unit (BLU), occurs in metasedimentary-metavolcanic (felsic-dominated) rocks on the Fennoscandian Shield in south-central Sweden. The mining district hosts a variety of ore deposit types including polymetallic Zn-Pb-Ag-(Cu-Au) deposits, with two end-member types being recognised by Allen *et al.* (1996): 1. Bedded stratiform Zn-Pb-Ag-rich sulphide mineralisation within rhyolitic ash-siltstone spatially associated with skarn, marble and metamorphosed sedimentary rocks (SAS-type); and 2. Stratabound, stacked sulphide lenses hosted in limestone-skarn and adjacent volcanic/volcaniclastic rocks (SVALS-type). SAS-type deposits include the large Zinkgruvan deposit (17.4 Mt @ 7.8 % Zn, 3.3 % Pb, 73 ppm Ag and 3.4 Mt @ 2.1 % Cu 33 ppm Ag, measured and indicated resources as of 2023, <https://lundinmining.com/operations/reserves-and-resources>, Hedström *et al.* 1989, Jansson *et al.* 2018), and the smaller Lovisa deposit (1.2 Mt @ 9.4 % Zn, 5.3 % Pb and 10–20 ppm Ag; Jansson *et al.* 2018). The more common SVALS-type deposits include the giant Garpenberg deposit with reserves (as of 2022) of 109 Mt @ 2.6 % Zn, 1.2 % Pb, 0.04 % Cu, 87 ppm Ag and 0.29 ppm Au; Falun (28.1 Mt @ 2–4 % Cu, 4 % Zn, 1.5 % Pb, 13–25 ppm Ag and  $\sim 3$  ppm Au, Allen *et al.* 1996); Sala (5 Mt @ 150–> 3,000 ppm Ag, 12 % Zn and 1.5 % Pb; Allen *et al.* 1996; Jansson 2017; Jansson *et al.* 2021); and Svärdsjö (1 Mt @ 6.0 % Zn, 2.7 % Pb, 0.62 % Cu and 112 ppm Ag, Ripa *et al.* 2015; Fahlvik *et al.* 2022).

There are various genetic theories regarding the formation of SVALS-type deposits including Broken Hill-type (BHT), skarn, volcanogenic massive sulphide (VMS) and sedimentary exhalative (SEDEX) models. However, studies by Allen *et al.* (1996) and Jansson *et al.* (2013, 2021) suggest they form a continuum between syn-volcanic, sub-seafloor replacement deposits and intrusion-related metasomatic Zn skarn deposits such as Sala. In contrast, SAS-type deposits are interpreted as metamorphosed SEDEX-like deposits and hybrid SEDEX-VMS

© The Author(s), 2024. Published by Cambridge University Press. This is an Open Access article, distributed under the terms of the Creative Commons Attribution licence (<http://creativecommons.org/licenses/by/4.0/>), which permits unrestricted re-use, distribution and reproduction, provided the original article is properly cited.



deposits that formed in or above the volcanic successions from basinal brines (e.g. Allen *et al.* 1996; Jansson *et al.* 2017, 2018).

Genetic considerations for some SVALS- and SAS-type deposits are, in part, based on light stable isotope (S, C and O) studies. Specifically, sulphur isotope studies have been carried out on the Falun (Gavelin *et al.* 1960), Gruvåsen (Hellingwerf & van Raaphorst 1988), Svärdsjö (Billström 1985), Zinkgruvan (Billström 1991; Jansson *et al.* 2017), Hällefors (Wagner *et al.* 2005), Lovisa (Jansson *et al.* 2018) and Sala deposits (Jansson *et al.* 2021). Three survey studies of C and O isotopes have been conducted on carbonates spatially associated with polymetallic sulphide deposits in the Bergslagen district. Billström *et al.* (1985) evaluated the C and O isotope compositions of carbonates in several deposits spatially associated with marbles, including a limited number of analyses of carbonates from the Stollberg, Sater and Saxberget SVALS-type deposits. They also included single C and O isotope compositions of carbonates from several other base metal occurrences and suggested that they could be used for exploration purposes. The survey study of De Groot and Sheppard (1988) concerned the C and O isotopic compositions of calcite and dolomite in stratabound carbonates, patches of carbonates in skarn deposits and carbonate veins, while Jonsson and Boyce (2002) conducted a C and O isotope study of dolomitic marbles and calcite within ore, and calcite veins in skarn ore in the Långban area. Other C and O isotope studies of massive sulphide deposits in the Bergslagen district include that of Allen *et al.* (2003) of carbonates associated with the Garpenberg SVALS-type Zn-Pb-Cu-Ag deposit along with a more limited study by Gebeyehu and Vivallo (1991). Combined S, C and O isotopes compositions in the Bergslagen district are restricted to those of Jansson *et al.* (2021) on the sub-seafloor Zn-Pb-Ag skarn deposits in the Sala area and of Billström (1985) on the Svärdsjö deposit.

The importance of the effects of high-temperature metasomatic fluids and how they modified the C and O isotope composition of the metamorphosed dolomites and limestone (now marbles) spatially associated with sulphide mineralisation was emphasised by Billström *et al.* (1985), De Groot and Sheppard (1988), Jonsson and Boyce (2002) and Jansson *et al.* (2021). The current study extends these earlier studies by evaluating the C and O isotope compositions of calcite in three deposits (Dammerget, Tvistbo and Grängsgruvan), and the S isotope compositions of sulphides (sphalerite, pyrite, chalcopyrite and galena) in the Dammerget, Baklångan and Grängsgruvan deposits in the Stollberg ore field, as well as a single sample of chalcopyrite from the Grönkullan banded iron formation deeper in the stratigraphy. These locations were chosen because they are distributed around the Stollberg syncline and are considered representative of deposits in the ore field. The aims of the study are to consider to which the degree metasomatic or magmatic-hydrothermal processes have operated in the Stollberg area and whether metamorphic decarbonation of spatially associated metamorphosed limestone was important, the source of the sulphur in the ore field, and to expand on the conditions of ore formation proposed previously by Jansson *et al.* (2013) and Frank *et al.* (2019). In this study, comparisons will be made with stable isotope compositions obtained previously from the Bergslagen district to evaluate the commonality of sulphur sources for the district and the possible role metasomatic/magmatic-hydrothermal/metamorphic processes played in ore formation.

## 2. Regional geology

The BLU, a lithotectonic unit that forms part of the Svecokarelian orogen in the Fennoscandian shield, originated as a marine

intra-arc or back-arc basin on continental crust (e.g. Allen *et al.* 1996; Stephens & Jansson, 2020). It consists primarily of c. 1.91–1.89 Ga plutonic rocks (mainly granite, diorite, granodiorite and gabbro) that intruded a thick unit of mainly felsic volcanic rocks (pyroclastic flow deposits, ash silt-sandstone, volcanogenic sandstone, coherent lavas, subvolcanic intrusions and volcanoclastic mass flow deposits), which are underlain and overlain by a package of siliciclastic rocks consisting of argillite, turbidite, quartzite and conglomerate (e.g. Allen *et al.* 1996; Stephens & Jansson, 2020). Allen *et al.* (1996) showed that stromatolitic limestones and minor banded iron formations occurring as interbeds in the volcanic succession formed in shallow marine environments during pauses in volcanism. The BLU was metamorphosed primarily to the amphibolite facies with areas reaching greenschist and granulite facies, with local evidence of migmatization (e.g. Andersson *et al.* 1992; Stephens *et al.* 2009). The Bergslagen district was subjected to at least two periods of ductile deformation (Stephens *et al.* 2009; Beunk & Kuipers 2012) with shear zones and plutonic rocks bounding the supracrustal rocks to form inliers (e.g. Stephens & Bergmann 2020). Other than polymetallic SVALS- and SAS-type Zn-Pb-Ag-(Cu-Au) deposits, the Bergslagen district hosts thousands of banded iron formation, Mn oxide, Fe oxide skarn, Fe oxide, W skarn, granite-pegmatite-hosted Mo deposits and pegmatite-hosted deposits (Weihed *et al.* 2005; Allen *et al.* 2008; Stephens *et al.* 2009). Note the term ‘skarn’ in the present study refers to stratiform or stratabound calc-silicate rocks dominated by garnet, clinopyroxene and/or clinoamphibole without any implied genetic or spatial association to an igneous intrusion, as defined previously by Jansson *et al.* (2013).

## 3. Local geology of the Stollberg ore field

The Stollberg ore field, which extends for ~15 km, was mined intermittently for over six centuries until 1982. It produced ~ 6.65 Mt with ore grades ranging from 0.5–5 wt. % Zn, 0.5–15.6 wt. % Pb and 5–320 ppm Ag, for at least a dozen sulphide occurrences (Selinus, 1983; Ripa, 1996; Jansson *et al.* 2013; Table 1). These deposits were metamorphosed to the amphibolite facies (~560°–600° C and 2–3.5 kb, Beetsma, 1992) and occur around a regional structural feature known locally as the Stollberg syncline, which is a N-S trending, upright to steeply dipping, S-plunging, second-generation fold (F<sub>2</sub>) (Fig. 1). Like other SVALS-type deposits in the Bergslagen district, sulphides are spatially associated with bimodal felsic and mafic volcanic rocks and metamorphosed limestone. The felsic volcanic rocks are dominated by variably altered rhyolitic ash-siltstone and massive pumice deposits, whereas the intrusive rocks include granitoids, porphyritic metarhyolite, amphibolite and post-Svecokarelian dolerite dykes. At least nine deposits occur on the eastern side of the Stollberg syncline with Grängsgruvan occurring on the western side and Norrgruvan and Tvistbo being located at the northern end, near the hinge of the F<sub>2</sub> fold (Fig. 1). Mafic sills are interspersed throughout the stratigraphy associated with the syncline (Figs. 2 and 3). The sulphide deposits formed just after a major rhyolitic, volcanic eruption and the development of a submarine caldera (Jansson *et al.* 2013).

The deepest part of the stratigraphy occurs on the eastern side of the Stollberg syncline and consists of a thick sequence of a rhyolitic quartz-feldspar-phyric volcanoclastic sandstone and magnetite skarn (Jansson *et al.* 2013). Note the term ‘phyric’ is used for volcanoclastic rocks in the Stollberg district with scattered larger phenocrysts in a fine-grained matrix as defined by Jansson *et al.* (2013). Overlying this package is the Staren limestone, which

**Table 1.** Characteristics of selected deposits in the Stollberg ore field

Deposit	Grade and tonnage	Metallic minerals	Ore zone minerals	Alteration types	References
Brusgruvan	Zn 3.2 wt%, Pb 15.6 wt%, Ag 320 ppm, Fe <1.23 wt%, Mn <0.10 wt%, As 13 ppm	Gn, Sp, Py	Qz, Flr, Mrc, Ms, Bt, Grs, Czo	Px skarn, Sil	M. Ripa (unpub. PhD thesis, Lund Univ. Lund, 1996), Jansson <i>et al.</i> (2013)
Stollgruvan	Zn 1-4 wt%, Pb 0.5-1 wt%, Ag 10 ppm, Fe 20-35 wt%, Mn 7 wt%, As <2786 ppm	Sp, Gn, Mag, Apy, Pyh, Py	Qz, Flr, Ms, Bal, Bt, Alm, Sps, Ghn, St, Crd, Hd, Ath, Tr, Ged, Chl, Ilm, Dsp	Ged-Ab, Grt-Bt, Px skarn	M. Ripa (unpub. PhD thesis, Lund Univ. Lund, 1996), Jansson <i>et al.</i> (2013)
Dammerberget	Zn 3-5 wt%, Pb 2-5 wt%, Ag 20-60 ppm, Fe 10 wt%	Sp, Gn, Mag, Apy, Pyh, Py	Qz, Flr, Ms, Bt, Cal, Phl, Chl, Hbl, Ath, Gru, Alm, Sps, Ol, Hd, Ilm, Tlc, Ghn	Ged-Ab, Px skarn, Grt-Bt	M. Ripa (unpub. PhD thesis, Lund Univ. Lund, 1996)
Baklängen	Zn 2.6 wt%, Pb 4.8 wt%, Ag 43 ppm, Fe <26.20 wt%, Mn <3.49 wt%, As <450 ppm	Mag, Sp, Gn, Pyh, Apy	Qz, Flr, Ms, Cal, Bt, Alm, Sps, Cam, Ol, Hu, Ghn, Grs, Hd, Chl, Ilm, Dsp, Alm	Ged-Ab, Qz-Bt, Grt-Amp-Ghn-Bt, Cam-Grt-Ghn-Flr skarn, Cam-Cpx skarn	Jansson <i>et al.</i> (2013), Månsson (1979)
Korrgruvan-Myggruvan	Zn 0.5 wt%, Pb 0.5 wt%, Ag 5 ppm, Fe 35 wt%, Mn 11 wt%, As <158 ppm	Mag, Sp, Gn, Pyh, Apy	Qz, Flr, Mrc, Ms, Cal, Bt, Alm, Sps, Cam, Hd, Ath, Chl, Ilm	Aed-Ab, skarn	Jansson <i>et al.</i> (2013)
Lustigkulla-Marnäs	Zn 1 wt%, Pb 0.5 wt%, Ag <2.8 ppm, Fe 30-40 wt%, Mn 10-15 wt%, As <3484 ppm	Sp, Gn, Mag, Apy, Lö, Pyh, Py	Qz, Flr, Ms, Cal, Bt, Alm, Sps, Cam, Gru, Hd, Chl, Ilm	Bt-Qz, Grt-Amp-Ghn-Bt, Cam-Grt-Ol-Flr, Cam-Cpx	M. Ripa (unpub. PhD thesis, Lund Univ. Lund, 1996), Jansson <i>et al.</i> (2013)
Grängsgruvan	6.65 Mt, Zn 7.7 wt%, Pb 2.6 wt%, Ag 60 ppm	Sp, Gn, Ccp, Py, Pyh	Qz, Bt, Phl, Ms, Chl, Kfs, Mrc, Pl, Hbl, Act, Alm, Sps, Cal, Cpx, Ep	Crd-Bt, Qz-Grt-Px, Ms, Sil, Grt-Bt	Raat <i>et al.</i> (2013), Frank <i>et al.</i> (2019)
Twistbo	575 kt, Zn 3.3 wt%, Pb 2.6 wt%, Ag 22 ppm	Sp, Gn, Ccp, Pyh, Mag	Qz, Bt, Phl, Ms, Chl, Kfs, Alm, Cpx, Cal, Ep	Grt-Bt, Px skarn, Qz-Grt-Px, Sil, Ms	Frank <i>et al.</i> (2019)
Norrgruvan	No data	Gn, Sp, Py, Pyh, Ccp, Au	Qz, Flr Bt, Ms, Chl, Mrc, Pl, Grt, Cam	Px skarn, Qz-Flr, Grt-Bt, Sil	Frank <i>et al.</i> (2019)

Abbreviations after Warr (2021).

is a calcite marble locally altered to skarn. This, in turn, is overlain by limestone and rhyolite breccias, and conglomerates that are interbedded with limestone (Jansson *et al.* 2013). This group of rocks is referred to as the Staren succession and is overlain by a 0.5 km thick unit of weakly altered feldspar + quartz-phyric pumice breccia-sandstone. Stratigraphically higher in the sequence is the so-called Stollberg limestone consisting of metamorphosed felsic volcanoclastic rocks, skarn and interbedded limestone that is hydrothermally altered near sulphide and magnetite mineralisation (Jansson *et al.* 2013). Above the Stollberg ore trend, a thick package of bedded rhyolitic ash silt-sandstone, with local beds of pumice and lithic breccia fills the upper part of the Stollberg syncline. These hanging wall rocks to the sulphide mineralisation contain calc-silicate aggregates and local coarse accumulations of cordierite, andalusite and muscovite. Further details of the stratigraphy and lithology on the eastern side of the syncline are given in Ripa (2012) and Jansson *et al.* (2013), while those for the deposits on the western side and northern end are given in Frank *et al.* (2019).

Sulphides occur in semi-massive zones, as disseminations and in veinlets with the dominant metallic minerals consisting of sphalerite, galena, chalcopyrite, pyrrhotite, pyrite, arsenopyrite and magnetite, along with rare gahnite (Table 1). Carbonates (mainly calcite) occur in marble units and in metamorphosed altered rocks as veins and clots. Ripa (2012) identified sulphide zonation in deposits on the eastern limb of the Stollberg syncline (herein referred to as the eastern deposits) with sphalerite and

galena being dominant in metalimestone, whereas chalcopyrite and pyrrhotite mainly occur in metarhyolite. A notable difference in the sulphide mineralogy for Grängsgruvan versus the eastern deposits is the high ratio of pyrite to pyrrhotite in the former; pyrrhotite is the dominant Fe sulphide in all other deposits in the Stollberg ore field. The metamorphosed altered rocks spatially related to the different deposits varies around the ore field. On the eastern side of the Stollberg syncline, a prominent zone of gedrite-albite rock occurs beneath the Dammerberget, Baklängen, Stollberg and Korrgruvan-Myggruvan deposits (Fig. 2). A unit up to 20 m wide consisting of a porphyroblastic garnet-amphibole-biotite  $\pm$ gahnite  $\pm$ cordierite  $\pm$ andalusite  $\pm$ sillimanite rock occurs immediately above some of the eastern deposits, where it is especially well exposed at Stollgruvan (Ripa, 1994; Jansson *et al.* 2013). Metamorphosed altered rocks spatially associated with sulphides include quartz-garnet-pyroxene, cordierite-biotite, garnet-biotite rock, skarn, siliceous and sericitic rocks, with the last two alteration styles being prominent at the Grängsgruvan deposit (Fig. 3).

The timing relationships between skarn formation, sulphide formation and regional metamorphism are complex. Recent local observations in the Stollberg ore field by us suggest that massive salite (i.e. ferroan diopside) skarn pre-dates both massive semi-massive magnetite and sulphide mineralisation. However, observations elsewhere of sphalerite, galena, pyrrhotite, chalcopyrite, arsenopyrite and pyrite as inclusions in porphyroblasts of garnet and hedenbergite (Jansson *et al.* 2013) suggest that sulphides were introduced prior to the formation of these anhydrous

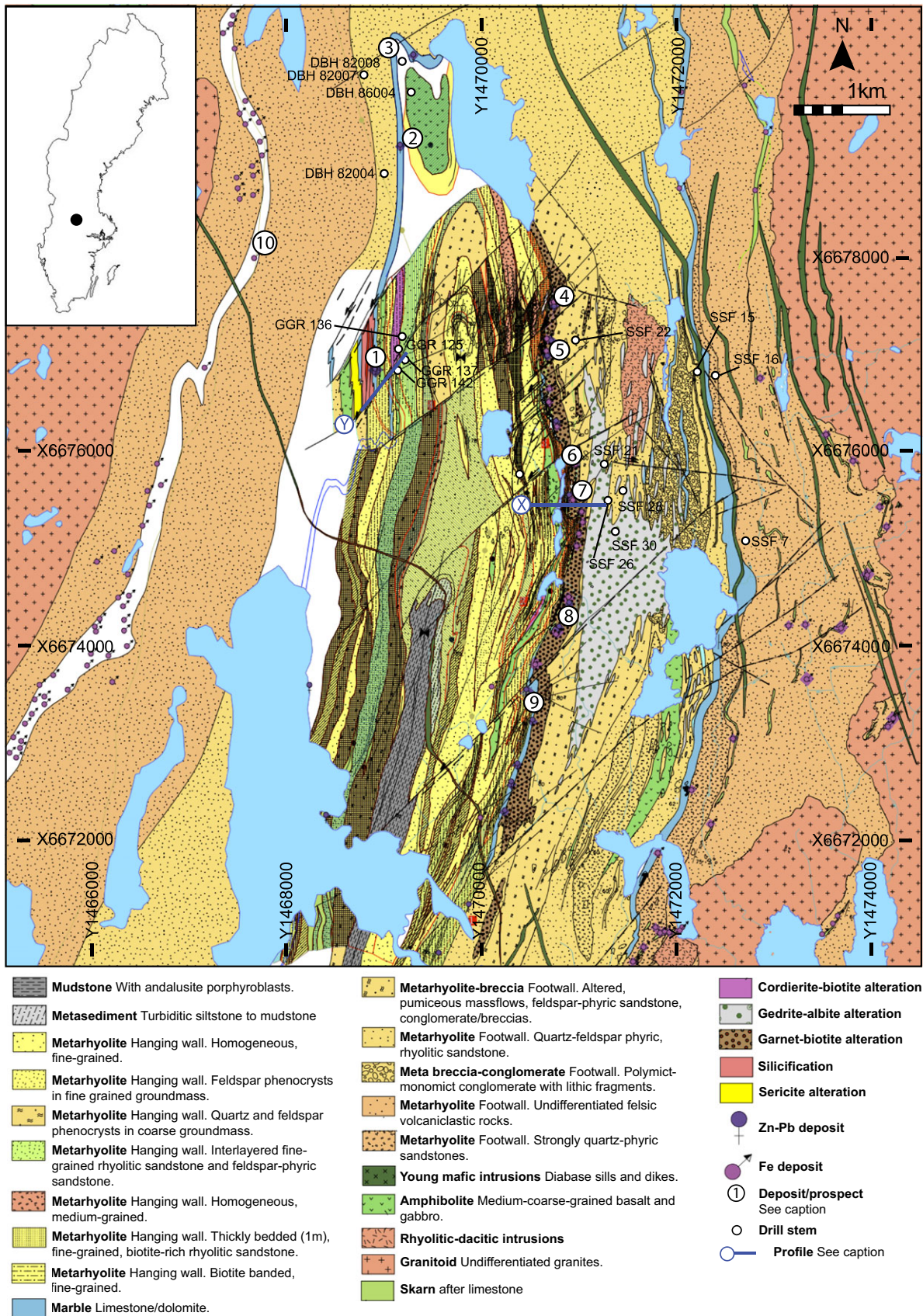


**Figure 1.** Geologic map of the Stollberg area, showing the location of mines, mineral occurrences and drill cores. 1 = Grängsruvan, 2 = Norrgruvan, 3 = Tvistbo, 4 = Lustigkullagruvan, 5 = Cedercreutz, 6 = Baklängen, 7 = Dammerget, 8 = Stollmalmen, 9 = Brusgruvan, 10 = Grönkullan. Drill cores from which samples were taken are shown. Grid is Swedish National Grid RT90, and inset map shows location of Stollberg in Sweden. Key provided on following page. Modified after Raat et al. (2013).

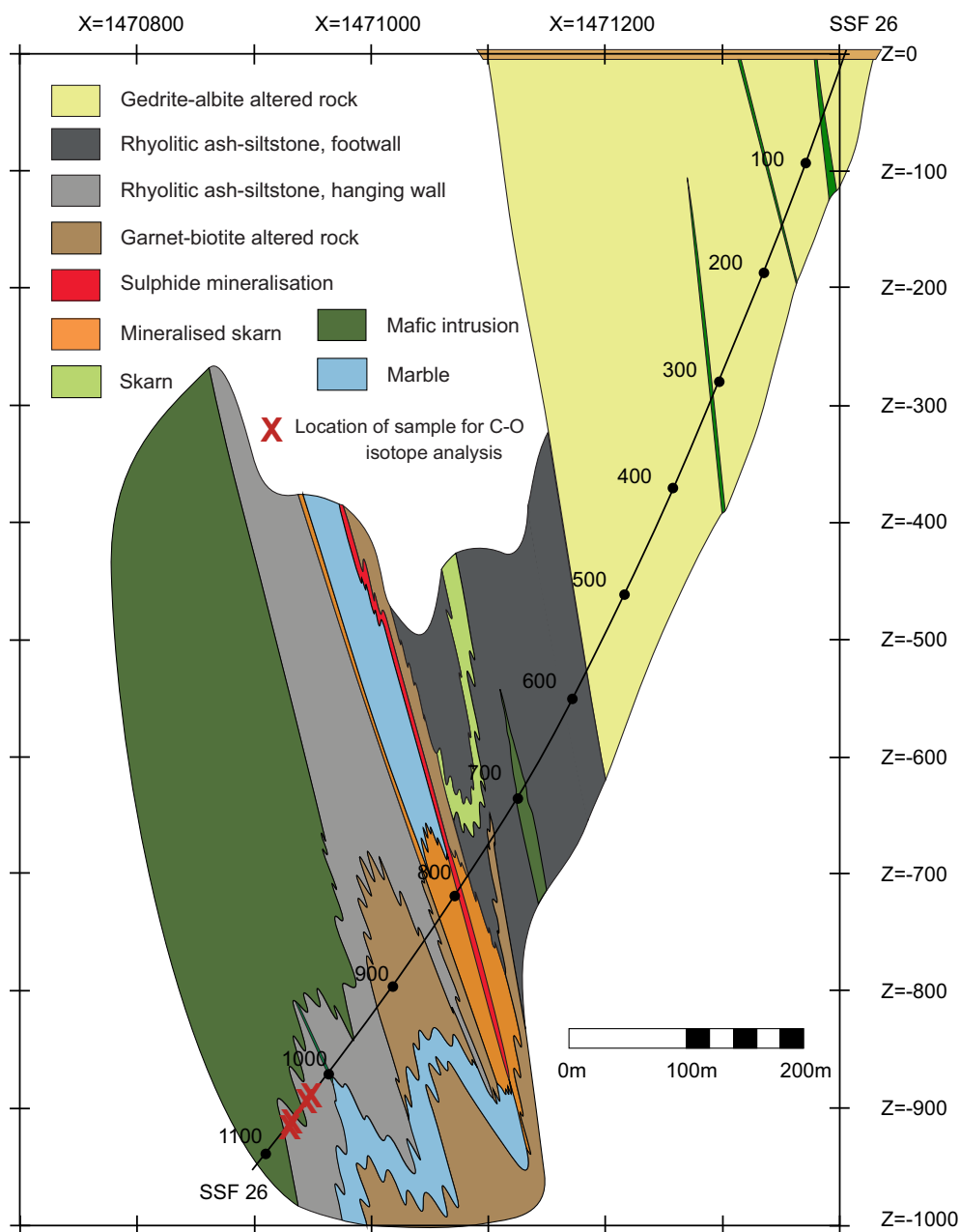


**Figure 2.** Geologic cross-section of the Dammerberget deposit along grid coordinate 6675600, shown as Profile Y in Figure 2. Drill core SSF 26 intersects this cross-section and shows the location of C and O isotope samples. Grid is Swedish National Grid RT90.

silicates. Syn-tectonic sulphide remobilisation is prevalent in the entire district which along with the lack of absolute ages for skarn silicates complicates interpretation and precludes generalisations. Specifically, it is unclear to what extent sulphides overprinting salite skarns represent syn-retrograde metamorphic, remobilised mineralisation cross-cutting peak metamorphic assemblages, or whether this cross-cutting relationship is a relict temporal feature of an original, premetamorphic mineral system where barren early anhydrous skarns were overprinted by sulphide-bearing, hydrous skarns.

Based on the variations in mineralogy and bulk rock compositions of skarn (i.e. Al-rich and Al-poor) spatially associated with sulphide mineralisation, Jansson *et al.* (2013) and Frank *et al.* (2019) suggested that skarn in the Stollberg ore field formed as a result of isochemical regional metamorphism of variable mixtures of limestone, rhyolite and iron oxides with the Al-rich skarns

containing a higher proportion of hydrothermally altered rhyolite. Detailed descriptions of the metamorphosed altered rocks are given in Ripa (1988, 1994, 2012), Björklund (2011), Jansson *et al.* (2013), Raat *et al.* (2013) and Frank *et al.* (2019, 2022).

#### 4. Analytical methods

Conventional sulphur isotopic analyses of sulphide powders for 41 samples (along with two duplicate analyses from the same sample) from drill core, obtained by crushing hand-picked sulphide grains using a binocular microscope, were performed via elemental analyser-continuous flow isotope ratio mass spectrometry (Studley *et al.* 2002) at the Indiana University Stable Isotope Research Facility. About 1-2mg of  $V_2O_5$  and the sample powder (0.1–0.2 mg) were loaded into tin cups, combusted in an elemental analyser to form  $SO_2$  and analysed in a Finnigan

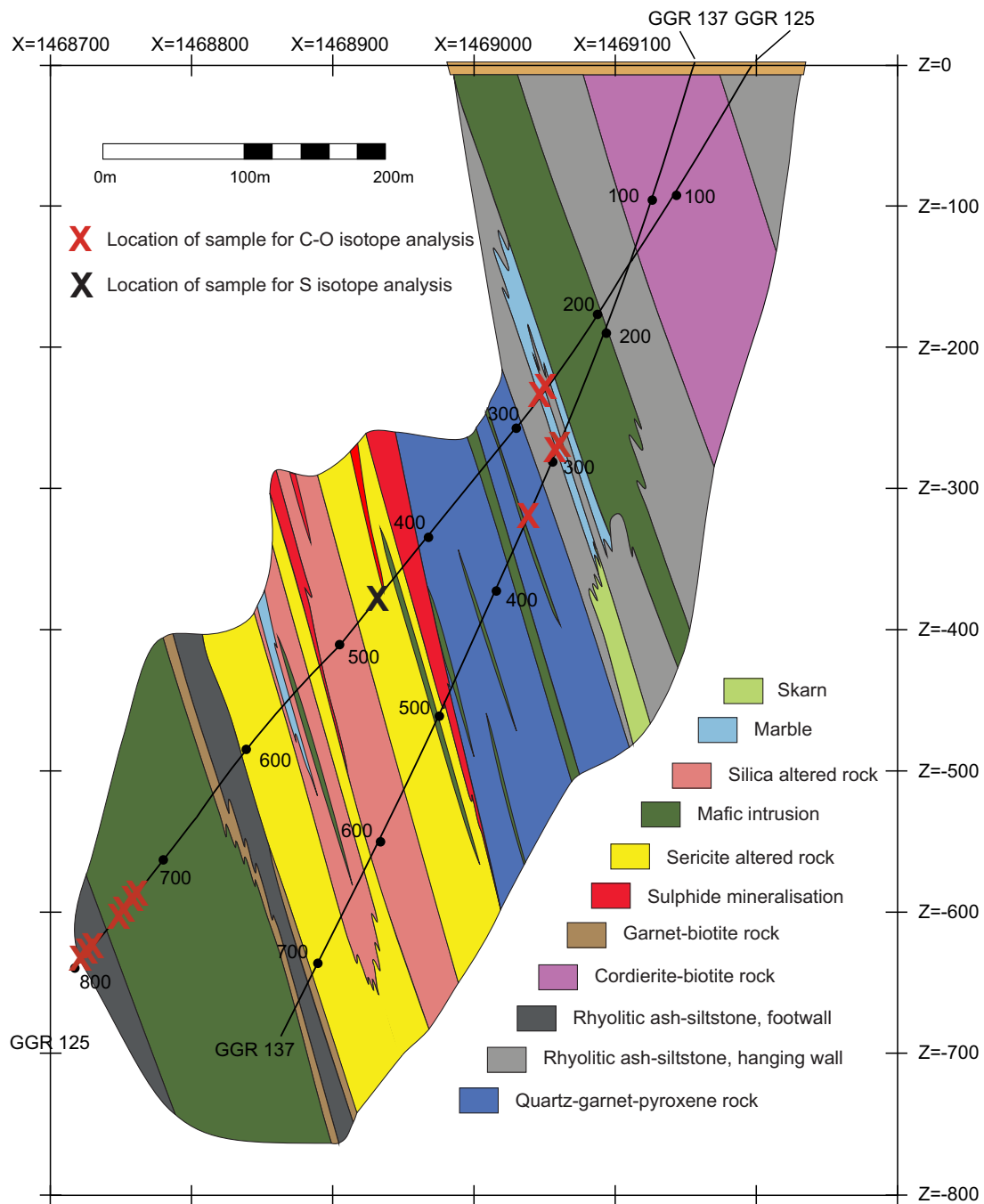


**Figure 3.** Geologic cross-section of the Grängsgruvan deposit along grid coordinate 6677050, shown as Profile X in Figure 2. Drill cores GGR 125 and GGR 137 intersect this cross-section. The location of S, C and O isotope samples are indicated. Grid is Swedish National Grid RT90.

Delta V stable isotope ratio mass spectrometer. International standards NBS-127, IAEA S-1, IAEA S-2 and IAEA S-3 with values of  $\delta^{34}\text{S} = +20.3\text{‰}$ ,  $-0.3\text{‰}$ ,  $+21.7\text{‰}$  and  $-31.3\text{‰}$  on the  $\text{SO}_2$ -scale were used as reference standards. Sample reproducibility determined by multiple analyses of standards is  $\pm 0.2\text{‰}$ ; instrumental measurement uncertainty is less than  $0.05\text{‰}$ . Results are given relative to Vienna Canyon Diablo troilite (VCDT) (Table 2).

Carbon and oxygen isotope compositions were obtained from 23 samples of calcite from drill core and followed a modified  $\text{CO}_2$  extraction method of McCrea (1950). Up to 2.7 mg of sample was reacted with  $\text{H}_3\text{PO}_4$  at  $50\text{ °C}$  in He-flushed vials. The released  $\text{CO}_2$

was measured in a Finnigan MAT Delta Plus XL mass spectrometer in continuous flow mode connected to a Gas Bench with a CombiPAL autosampler housed in the Department of the Earth, Atmosphere and Climate, Iowa State University. At least one reference standard was used for every five samples. Results given in Table 3 are relative to Vienna Pee Dee Belemnite (VPDB) and Standard Mean Ocean Water (VSMOW). The combined uncertainty (analytical uncertainty and average correction factor) for  $\delta^{13}\text{C}$  is  $\pm 0.05\text{‰}$  (VPDB) and  $\delta^{18}\text{O}$  is  $\pm 0.06\text{‰}$  (VPDB/SMOW), respectively, on the basis of two internal standards calibrated against primary reference standards (NBS-18, NBS-19, LSVEC).

**Table 2.** Sulphur isotope compositions of sulphides from the Stollberg ore field

Deposit	Sample name	Mineral	Rock type	$\delta^{34}\text{S}$ (‰ VCDT)
Gränsgruvan	GGR125-476.1	Pyrite	Pyrite-pyrrhotite vein in quartz-sericite-pyrite rock	+2.99
Gränsgruvan	GGR125-476.1	Pyrrhotite	Pyrite-pyrrhotite vein in quartz-sericite-pyrite rock	+2.18
Gränsgruvan	GGR136-336.5	Pyrrhotite	Pyrrhotite intergrown with Gn and Sp in quartz-garnet-pyroxene rock	+3.41
Gränsgruvan	GGR136-351.1	Sphalerite	Sphalerite in sulphide mineralisation in rhyolitic ash silt-sandstone	+3.11
Gränsgruvan	GGR136-352.9	Sphalerite	Sphalerite intergrown with pyrite in rhyolitic ash silt-sandstone	+3.07
Gränsgruvan	GGR136-361.5	Sphalerite	Sphalerite in sulphide mineralisation in rhyolitic ash silt-sandstone	+2.33
Gränsgruvan	GGR136-362.6	Pyrite	Pyrite in sulphide zone in rhyolitic ash silt-sandstone	+3.14
Gränsgruvan	GGR136-389.3	Pyrite	Pyrite in sulphide zone in rhyolitic ash silt-sandstone	+4.47
Gränsgruvan	GGR136-396.6	Sphalerite*	Sphalerite in sulphide zone in rhyolitic ash silt-sandstone	+2.83
Gränsgruvan	GGR136-423.6	Pyrite	Pyrite in siliceous rhyolitic ash silt-sandstone	+2.12
Gränsgruvan	GGR136-442.5	Pyrite	Pyrite in siliceous rhyolitic ash silt-sandstone	+2.41
Gränsgruvan	GGR136-445.2	Pyrite	Pyrite in siliceous rhyolitic ash silt-sandstone	+2.91
Gränsgruvan	GGR136-449.0	Pyrite	Pyrite in siliceous rhyolitic ash silt-sandstone	+3.71
Gränsgruvan	GGR136-458.6	Pyrite	Pyrite in siliceous rhyolitic ash silt-sandstone	+2.25
Gränsgruvan	GGR136-467.7	Pyrite	Pyrite in siliceous rhyolitic ash silt-sandstone	+2.64
Gränsgruvan	GGR136-511.4	Pyrite	Pyrite in siliceous rhyolitic ash silt-sandstone	+3.46
Gränsgruvan	GGR138-440.8	Pyrrhotite	Cm-wide vein of pyrrhotite in phlogopite-sericite-pyrite rock	+2.59
Gränsgruvan	GGR138-446.7	Pyrite	Pyrite vein in phlogopite-sericite-pyrite rock	+4.23
Gränsgruvan	GGR138-471.4	Pyrite	Pyrite vein in phlogopite-sericite-pyrite rock	+2.38
Gränsgruvan	GGR138-494.2	Pyrite	Massive pyrite in Py-Pyh-Mag-Ccp in phlogopite-sericite-quartz rock	+3.14
Gränsgruvan	GGR142- 460.1	Pyrite	Coarse pyrite with trace Pyh, Sp, and Ccp in sericite-quartz-pyrite rock	+3.17
Gränsgruvan	GGR142-418.5	Pyrite	Coarse pyrite in quartz-phlogopite rock	+3.72
Gränsgruvan	GGR142-420.0	Pyrite	Pyrite in in sericite-phlogopite rock	+2.15
Gränsgruvan	GGR142-423.4	Pyrite	Coarse pyrite in quartz-phlogopite rock (zone of massive sulphides)	+3.74
Gränsgruvan	GGR142-428.8	Pyrite	Coarse pyrite in quartz-sericite-phlogopite rock	+4.63
Gränsgruvan	GGR142-429.7	Pyrite	Coarse pyrite in quartz-sericite-phlogopite rock	+3.49
Gränsgruvan	GGR142-441.7	Pyrite	Pyrite in coarse pyrite-quartz vein with minor Ccp in quartz-sericite rock	+3.94
Gränsgruvan	GGR142-447.8	Pyrite	Coarse pyrite in quartz-sericite rock	+2.13
Gränsgruvan	GGR142-472.5	Sphalerite	Coarse sphalerite vein in quartz-sericite-pyrite rock	+3.51
Gränsgruvan	GGR142-478.3	Pyrite	Coarse pyrite vein in quartz-sericite-pyrite rock	+4.54
Grönkullan	Green Hill 1	Chalcopyrite*	Chalcopyrite in skarn-bearing iron formation	-14.02
Baklängen	SSF21-408.5	Pyrrhotite	Pyrrhotite in garnet-biotite-hedenbergite skarn	+3.93
Baklängen	SSF21-418.6	Pyrrhotite	Massive pyrrhotite in skarn	+4.34
Dammberget	SSF28-740.7	Pyrite	Pyrite in quartz vein in rhyolitic ash silt-sandstone	+5.71
Dammberget	SSF28-741.2	Pyrrhotite	Pyrrhotite in quartz vein in rhyolitic ash silt-sandstone	+3.82
Dammberget	SSF28-861.6	Pyrrhotite	Pyrrhotite in massive sulphides in skarn	+4.80
Dammberget	SSF28-864.6	Sphalerite	Sphalerite in massive sulphides in skarn	+4.33
Dammberget	SSF28-866.1	Pyrrhotite	Pyrrhotite in massive sulphides in skarn	+3.43
Dammberget	SSF28-884.5	Galena	Galena in marble	+2.96
Dammberget	SSF30-507.0	Pyrrhotite	Pyrrhotite in pyrrhotite-chalcopyrite quartz vein	+4.91
Dammberget	SSF30-593.9	Pyrrhotite	Pyrrhotite in quartz vein in garnet-biotite rock	+5.69

\*Average of duplicate analyses.  
Abbreviations after Warr (2021).

**Table 3.** Carbon and oxygen isotope compositions of calcite from the Stollberg district

Deposit	Drill core	Lithology	$\delta^{13}\text{C}$ (VPDB)	$\delta^{18}\text{O}$ (SMOW)	$\delta^{18}\text{O}$ (VPDB)
Tvistbo	DBH 82008 105.50	Skarn	-0.30	+10.82	-19.49
Tvistbo	DBH 82008 107.50	Skarn	-0.59	+11.15	-19.17
Tvistbo	DBH 82008 108.00	Skarn	-0.79	+10.32	-19.81
Tvistbo	DBH 82008 155.80	Skarn	-9.41	-6.89	-36.66
Tvistbo	DBH 82008 156.50	Skarn	-3.22	+9.69	-20.59
Tvistbo	DBH 82008 160.20	Skarn	-0.11	+10.55	-19.75
Tvistbo	DBH 82008 171.90	SBS	-1.93	+10.70	-19.61
Grängsgruvan	GGR 125 269.10	Marble	-3.91	+12.40	-17.95
Grängsgruvan	GGR 125 269.20	Marble	-4.90	+9.08	-21.18
Grängsgruvan	GGR 125 743.70	Mafic	-2.44	+11.08	-19.24
Grängsgruvan	GGR 125 758.20	Mafic	+0.11	+11.69	-18.64
Grängsgruvan	GGR 125 760.00	Mafic	-3.01	+10.80	-19.50
Grängsgruvan	GGR 125 763.40	Mafic	-2.02	+10.64	-19.66
Grängsgruvan	GGR 125 783.30	RAS	+0.57	+11.91	-18.43
Grängsgruvan	GGR 125 789.20	RAS	+0.75	+13.40	-16.98
Grängsgruvan	GGR 125 789.80	RAS	+0.43	+10.52	-19.78
Grängsgruvan	GGR 137 297.80	Marble	-0.30	+10.87	-19.44
Grängsgruvan	GGR 137 302.00	Marble	-2.41	+10.36	-19.94
Grängsgruvan	GGR 137 340.20	QGP Rock	-5.46	+8.91	-21.34
Dammberget	SSF 26 1038.20	RAS	-2.09	+10.10	-20.18
Dammberget	SSF 26 1038.30	RAS	-1.83	+14.06	-16.35
Dammberget	SSF 26 1049.00	RAS	-2.10	+10.01	-20.27
Dammberget	SSF 26 1051.30	RAS	-0.66	+12.25	-18.01

SBS, sulphide-bearing biotite schist; RAS, rhyolitic ash silt-sandstone; QGP, quartz-garnet-pyroxene altered rock.

## 5. Results

The sulphur isotope compositions of sulphides from the Stollberg ore field are shown in Table 2 and Figure 4. Of the 41 samples analysed here, 30 were of sulphides (pyrite, pyrrhotite and sphalerite) from the Grängsgruvan deposit, with all but one sample (GGR136 336.5, a quartz-garnet-pyroxene rock) derived from veins/veinlets, masses or disseminations in rhyolitic ash silt-sandstone, sericite-altered rocks or siliceous altered rock. Samples from Grängsgruvan have the following isotopic values:  $\delta^{34}\text{S}_{\text{pyrite}} = +2.12$  to  $+4.54$  ‰,  $n = 22$ ;  $\delta^{34}\text{S}_{\text{pyrrhotite}} = +2.18$  to  $+3.41$  ‰,  $n = 3$ ;  $\delta^{34}\text{S}_{\text{sphalerite}} = +2.33$  to  $+3.51$  ‰,  $n = 5$ , whereas those from Dammberget show values of  $\delta^{34}\text{S}_{\text{pyrite}} = +5.71$  ‰,  $n = 1$ ;  $\delta^{34}\text{S}_{\text{pyrrhotite}} = +3.82$  to  $+5.69$  ‰,  $n = 4$ ;  $\delta^{34}\text{S}_{\text{sphalerite}} = +4.33$  ‰,  $n = 1$ ;  $\delta^{34}\text{S}_{\text{galena}} = +2.96$  ‰,  $n = 1$ ). Two samples of pyrrhotite from the Baklängen deposit have values of  $\delta^{34}\text{S}_{\text{pyrrhotite}} = +3.93$  and  $+4.34$  ‰, whereas a sample of chalcopyrite in iron formation from Grönkullan has a very light isotopic value of  $\delta^{34}\text{S}_{\text{chalcopyrite}} = -14.02$  ‰. Given this anomalous value, relative to all the other samples analysed here, this sample was reanalysed to check whether there was an unforeseen problem with the analytical procedure. However, the same value (-14.00 ‰ and -14.04 ‰) was obtained within analytical uncertainty. The average sulphur isotopic values for samples from Grängsgruvan, Dammberget and Baklängen are  $\delta^{34}\text{S} = +3.15$  ‰ ( $n = 30$ ),  $+4.46$  ‰ ( $n = 8$ ) and  $+4.14$  ‰ ( $n = 2$ ), respectively, which are similar regardless

of the composition of the sulphide and the number of samples analysed.

Carbon and oxygen isotope compositions of calcite are shown in Table 3 and were obtained in skarn and sulphide-bearing schist from the Tvistbo deposit ( $\delta^{13}\text{C} = -9.41$  to  $-0.11$  ‰;  $\delta^{18}\text{O}_{\text{VSMOW}} = -6.89$  to  $+11.15$  ‰;  $n = 7$ ), marble, quartz garnet pyroxene altered rock, amphibolite and sulphide-bearing schist from Grängsgruvan ( $\delta^{13}\text{C} = -5.46$  to  $+0.75$  ‰;  $\delta^{18}\text{O}_{\text{VSMOW}} = +8.91$  to  $+13.40$  ‰;  $n = 12$ ) and sulphide-bearing schist from the Dammberget deposit ( $\delta^{13}\text{C} = -2.10$  to  $-0.66$  ‰;  $\delta^{18}\text{O}_{\text{VSMOW}} = +10.01$  to  $+14.06$  ‰;  $n = 4$ ). Sample DBH 82008 155.80, a skarn, is anomalous by comparison to other samples showing the lightest isotopic compositions ( $\delta^{13}\text{C} = -9.41$  ‰ and  $\delta^{18}\text{O}_{\text{VSMOW}} = -6.89$  ‰) of all samples analysed here.

## 6. Discussion

### 6.a. Source of sulphur and physicochemical conditions of formation of Stollberg sulphides

In evaluating the general physicochemical conditions of formation of SVALS-type deposits, Jansson *et al.* (2013) and Kampmann *et al.* (2017) suggested they formed from mineralising fluids that were acid, reducing and hot ( $> 250$  °C), in part, based on the feldspar-destructive alteration style associated with sulphide mineralization,



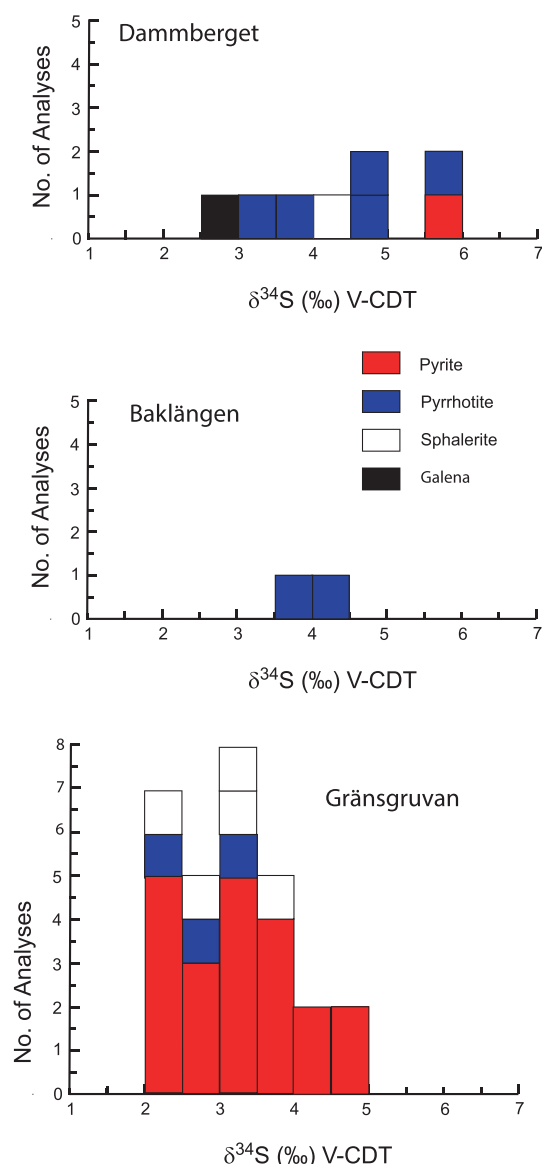


**Figure 4.** Histograms showing the sulphur isotope compositions of the Dammberget, Baklängen and Grängsgruvan deposits in the Stollberg ore field.

the presence of positive Eu anomalies in hydrothermal precipitates and the nature of the carbonate replacement/skarn formation. Jansson *et al.* (2021) proposed the temperature of the ore fluid at Sala was around 300 °C, while Kampmann *et al.* (2017) considered that associated with sulphide formation at Falun to have been approximately 300° to 400 °C.

The absence of organic material (i.e. graphite) in the ore-forming sequence at Stollberg makes bacteriogenic sulphate reduction (BSR) and thermochemical sulphate reduction (TSR) of seawater an unlikely source of sulphur. Instead, the ore-forming conditions are compatible with inorganic reduction of seawater sulphate. In an attempt to model the approximate log  $fO_2$  and pH conditions of the premetamorphic ore-forming fluid, information on T, ionic concentration of the ore fluid (I) and  $\delta^{34}S_{SS}$  are required (Ohmoto, 1972). Further constraints can be made on the ore-forming conditions by knowing the stabilities of members of the systems Fe-S-O and K-Al-Si-O-H. The assemblage magnetite-pyrrhotite-pyrite, which is common in the Stollberg ore field, is a

metamorphic assemblage, but there is no textural evidence to suggest that these three minerals did not precipitate from the premetamorphic ore-forming solution. In keeping with Jansson *et al.*'s (2013) assumption that the ore-forming fluid temperature in the Stollberg ore field was >250 °C, we have calculated possible premetamorphic conditions at temperatures of 250 ° and 350 °C in  $fO_2$ -pH space (Figs. 5 and 6). These figures have been drawn for values of  $\delta^{34}S_{SS} = +3$  ‰ and +17 ‰ (the latter assuming a 1.9 Ga seawater sulphate value of Claypool *et al.*, 1980),  $I = \sim 1$  m NaCl (approximate seawater salinity), and a total dissolved S content of 0.01 and 0.1 moles/kg  $H_2O$  at  $T = 250$  °C (Fig. 5), along with a total dissolved S content of 0.01 moles/kg  $H_2O$  at  $T = 350$  °C (Fig. 6). The presence of sericite, quartz, K-feldspar and pyrite in silica-altered rocks adjacent to the Grängsgruvan deposit (Frank *et al.* 2019) as well as the likely precursor of the porphyroblastic garnet-amphibole-biotite altered rock associated with some of the eastern deposits, which Ripa (1988) and Jansson *et al.* (2013) proposed was a sericite-chlorite-rich alteration zone, suggests that the ore-forming fluid was in the muscovite stability field close to or on the muscovite-K-feldspar equilibrium boundary (Figs. 5, 6). The sulphur isotopic compositions of pyrite are superimposed on Figures 5 and 6 noting that the range of isotopic compositions from the Stollberg ore field ( $\delta^{34}S = +1$  to +6 ‰) fall along contours that occur near the pyrite-pyrrhotite-magnetite triple point regardless of the temperature (250 ° or 350 °C) and the total dissolved S content chosen (0.01 or 0.1 moles/kg  $H_2O$ ) chosen. The stability field of the ore-forming fluid is further constrained by the stability of calcite, which is present in the ore. A value  $\delta^{34}S_{SS}$  of +3 ‰ may suggest a direct input from a magmatic source or from disseminated sulphides in the volcanoclastic pile associated with the ore trend. However, we also consider the possibility that the source of sulphur may have been entirely derived from contemporaneous Proterozoic seawater sulphate, without any contribution from an igneous source of sulphur, given that modified seawater was likely responsible for the widespread alteration associated with mineralisation. If a value of  $\delta^{34}S_{SS} = +17$  ‰ is applied to Figures 5 and 6 instead of  $\delta^{34}S_{SS} = +3$  ‰, contours for the values of  $\delta^{34}S = +1$  to +6 ‰ for Stollberg sulphides intersect the pyrite-magnetite join but never overlap the pyrrhotite stability field. Given that pyrrhotite is the most common member of the system Fe-S-O in metallic minerals in ore in the Stollberg ore field, notwithstanding the pyrite:pyrrhotite ratio > 1 at Grängsgruvan, would suggest for a value of  $\delta^{34}S_{SS} = +17$  ‰ that a premetamorphic ore-forming fluid was relatively oxidising and that the assemblage in the system Fe-S-O was pyrite-magnetite. If this was the case, then the premetamorphic assemblage would have to convert to pyrrhotite-magnetite and pyrite-pyrrhotite-magnetite during amphibolite facies metamorphism via the desulphidation of pyrite. It is more likely that the common presence of pyrrhotite in the Stollberg ore field is simply due to the premetamorphic ore assemblage being relatively sulphur-poor. This suggestion is consistent with the high abundance of iron oxides and iron silicates in the ore field (i.e. much Fe is not in sulphides), probably because the amount of sulphur was limited. Note also that there are other polymetallic sulphide deposits in the Bergslagen district (e.g. Falun, Garpenberg), which have been subject to amphibolite facies conditions, where pyrite is a stable metamorphic mineral and was not all converted to pyrrhotite. Regardless, primary premetamorphic pyrrhotite has not been observed at Stollberg. This may not be surprising given that pyrrhotite is such a ductile and mobile phase (Gilligan & Marshall, 1987). There are several examples in the Stollberg ore field where

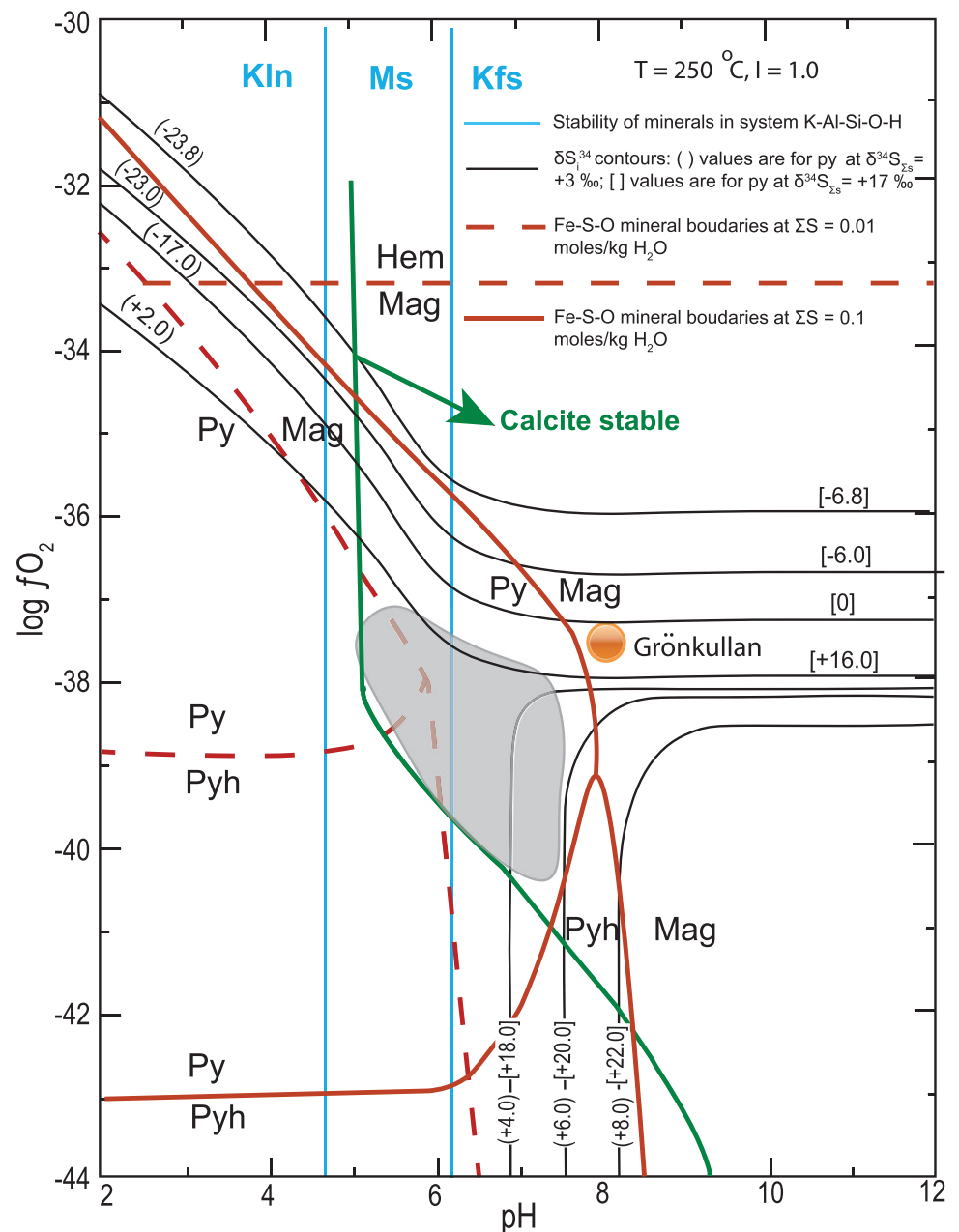


**Figure 5.** Isothermal  $\log fO_2$ -pH diagram for the stability of sulphides in the system Fe-S-O from the Stollberg ore district. Sulphur isotope contours for pyrite are drawn for  $T = 250^\circ\text{C}$ ,  $\delta^{34}\text{S}_{\Sigma\text{S}} = +3\text{‰}$  and  $+17\text{‰}$  (i.e. 1.9 Ga seawater sulphate value; Claypool, 1980), and  $I = 1.0$ . Minerals in the system Fe-S-O are shown for  $\Sigma\text{S} = 0.01$  moles/kg  $\text{H}_2\text{O}$  as red dashed lines and  $\Sigma\text{S} = 0.1$  moles/kg  $\text{H}_2\text{O}$  as red solid lines. The shaded region shows the approximate range of conditions for  $\delta^{34}\text{S}$  of pyrite over  $fO_2$ -pH range indicated given the presence of the assemblages: pyrite-pyrrhotite, pyrite-pyrrhotite-magnetite, pyrite-magnetite and magnetite-pyrrhotite, as well as calcite. The stability field of calcite is shown for  $\Sigma\text{C} = 1$  moles/kg  $\text{H}_2\text{O}$ . Also shown are the stability fields of minerals in the system K-Al-Si-O-H, based on data from Hemley (1959) where the abbreviations are Kln kaolinite, Ms muscovite and Kfs K-feldspar. The figure is modified after Ohmoto (1972). The orange circle shows the approximate position for the chalcopyrite sample from Grönkullan. It is positioned on the  $\delta^{34}\text{S} = -14\text{‰}$  contour for pyrite within the magnetite stability field.

tectonically remobilised pyrrhotite occurs in post- $D_2$  faults and fractures as well as in pressure shadows of silicate minerals. The one caveat to the idea that the ore fluid was relatively oxidising is that the anomalous value of  $\delta^{34}\text{S} = -14.02\text{‰}$  for chalcopyrite in iron formation from the Grönkullan sample can be accounted for by equilibration of chalcopyrite at higher  $fO_2$  conditions with magnetite/hematite (Figs. 5, 6). However, it must be stressed that Grönkullan occurs stratigraphically below the Stollberg ore field and may not belong to the same fluid system. Given that only one sample was analysed here, the isotopic value is an outlier and the conditions of formation of sulphides at Grönkullan warrant further investigation.

Regardless of the absence of an obvious spatially related igneous intrusion that may have been involved in the mineralising event, it cannot be ruled out that the ore system transitioned with time and burial to a metasomatic one probably involving magmatic-hydrothermal fluids. Nonetheless, despite this possibility, our

preferred model to explain the alteration associated with the mineralisation and the observed sulphur isotopic values is for heated modified seawater to have circulated through the volcanoclastic pile and to have assimilated disseminated sulphide.

#### 6.b. Metasomatism, subsea floor premetamorphic alteration or interaction with high-T fluids with carbonates at Stollberg?

When appraising the origin of limestones in the Stollberg ore field, Jansson *et al.* (2013) considered several possibilities based on textural and bulk rock geochemical data. For example, based on the presence of positive Eu anomalies in the Stollberg limestone, they suggested that the limestone could be a hydrothermal non-exhalative carbonate. They also considered the possibility that the limestone formed by microbial stromatolitic growth with a hydrothermal-exhalative component. In this regard, Jansson

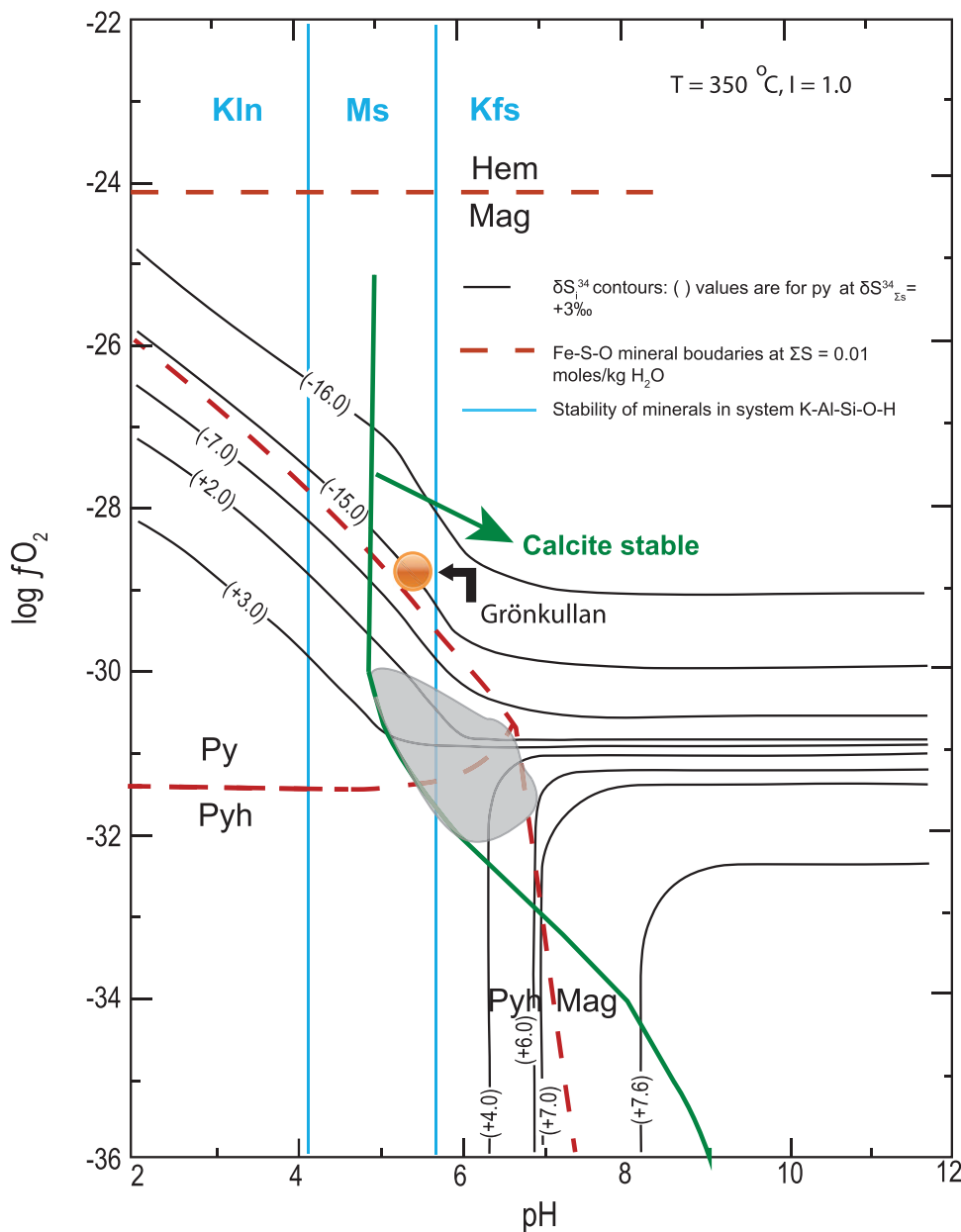


**Figure 6.** Isothermal  $\log fO_2$ -pH diagram for the stability of sulphides in the system Fe-S-O from the Stollberg ore district. Sulphur isotope contours for pyrite are drawn for  $T = 350\text{ }^\circ\text{C}$ ,  $\delta^{34}S_{\Sigma S} = +3\text{ }‰$  and  $I = 1.0$ . Minerals in the system Fe-S-O are shown for  $\Sigma S = 0.01$  moles/kg  $H_2O$  as red dashed lines. The shaded region shows the approximate range of conditions for  $\delta^{34}S$  of pyrite in  $fO_2$ -pH space given the presence of the assemblages: pyrite-pyrrhotite, pyrite-pyrrhotite-magnetite, pyrite-magnetite and magnetite-pyrrhotite, as well as calcite. The stability field for calcite is shown for  $\Sigma C = 3$  moles/kg  $H_2O$ . Also shown is the stability field of minerals in the system K-Al-Si-O-H, based on data from Hemley (1959) where the abbreviations are Kln kaolinite, Ms muscovite and Kfs K-feldspar. The figure is modified after Ohmoto (1972). The orange circle shows the approximate position for the chalcopyrite sample from Grönkullan. It is positioned on the  $\delta^{34}S = -14\text{ }‰$  contour for pyrite within the magnetite stability field.

*et al.* (2013) recognised that the Stollberg limestone bore resemblance to the well-described stromatolitic limestone at Sala (Allen *et al.* 2003; Jansson *et al.* 2021), even though primary stromatolitic textures have not been observed in the limestones at Stollberg. In places, the limestone contains elevated concentrations of Mn (i.e. percent levels), which is anomalous for metamorphosed limestones in the Bergslagen district. The presence of Mn along with the aforementioned positive Eu anomaly supports the concept of a hydrothermal-exhalative component to the limestone, possibly in the form of Ca+Mn carbonate. Alternatively, Jansson *et al.* (2013) opined that the elevated Mn and Eu concentrations of the limestone, which is locally dolomitic, may be the result of premetamorphic hydrothermal alteration of the limestone. Such Fe and Mn alteration has been demonstrated elsewhere in the Bergslagen district at Garpenberg by Allen *et al.* (2003) and at Sala by Jansson & Allen (2020) and Jansson *et al.* (2021).

In further considering the origin of carbonates at Stollberg, Jansson *et al.* (2013) noted that Billström *et al.* (1985) analysed the

C and O isotopic composition of four samples of the Stollberg limestone, which yielded values ranging from  $\delta^{13}C_{VPDB} = -2.3$  to  $-0.8\text{ }‰$  and  $\delta^{18}O_{VSMOW} = +9.5$  to  $+11.2\text{ }‰$ , and one sample from the Staren limestone showed values of  $\delta^{13}C_{VPDB} = -0.1\text{ }‰$ ,  $\delta^{18}O_{VSMOW} = +10.9\text{ }‰$ . The isotopic values obtained by Billström *et al.* (1985) overlap the range obtained here ( $\delta^{13}C_{VPDB} = -5.46$  to  $+0.75\text{ }‰$  and  $\delta^{18}O_{VSMOW} = +8.91$  to  $+14.06\text{ }‰$ ) (Fig. 7), although this range does not include a single sample of calcite in skarn from Tvistbo (DBH82008 155.80), which possesses extremely negative isotopic values for both C and O ( $\delta^{13}C_{VPDB} = -9.41\text{ }‰$  and  $\delta^{18}O_{VSMOW} = -6.89\text{ }‰$ ). Notwithstanding this sample, which is conceivably the result of analytical error, the C and O isotopic values of carbonate in the Staren limestone are close to the average isotopic values of Late Proterozoic (i.e. Orosirian) dolomite and calcite (Shields & Veizer 2002). About half of the samples analysed here show C isotopic composition close to average values of Late Proterozoic carbonates, while the remainder are isotopically lighter. Values of  $\delta^{18}O_{VSMOW}$  for carbonates analysed here are

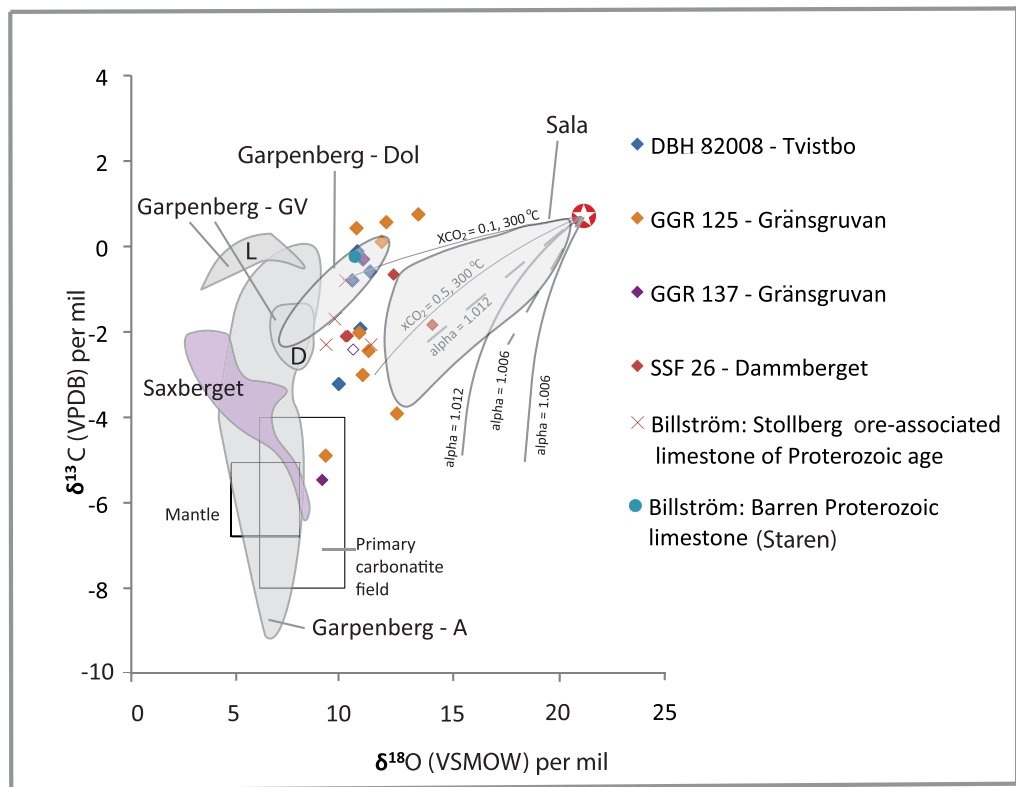


**Figure 7.** A plot of  $\delta^{13}\text{C}_{(\text{VPDB})}$  vs  $\delta^{18}\text{O}_{(\text{VSMOW})}$  for calcite samples from the Tvistbo, Grängsgruvan and Dammerberget deposits in the Stollberg ore field. A single anomalous sample (i.e. DBH 82008 155.80, a skarn, which exhibits the lightest isotopic compositions ( $\delta^{13}\text{C} = -9.41\text{‰}$  and  $\delta^{18}\text{O}_{\text{VSMOW}} = -6.89\text{‰}$ ) reported here is not shown. Drill hole numbers are shown for the Tvistbo, Grängsgruvan and Dammerberget deposits. Symbols of samples derived from unlocated ore-associated limestone samples and carbonate in the Staren limestones in the Stollberg ore field from Billström *et al.* (1985) are also shown. Note the isotopic compositions of these samples overlap with the data obtained here from Stollberg. Isotopic compositions from other SVALS-type deposits are also shown in the shaded areas: Garpenberg - A = calcite in mineralised skarn (Allen *et al.* 2003), Garpenberg - Dol = dolomite halo around mineralisation (Allen *et al.* 2003), Garpenberg - GV = limestone (L) and dolomite (D) associated with ore (Gebeyehu & Vivallo 1991), Saxberget = ore-associated limestone (Billström *et al.* 1985), and Sala = dolomite marble, calcite marble and calcite gangue associated with mineralisation (Jansson *et al.* 2021). Isotopic shifts are shown using the approach of Valley (1986) due to batch volatilisation (dashed grey lines) and Rayleigh volatilisation (solid grey lines). Modelling was done utilising fluid rock fractionation factors  $\alpha^{18}\text{O}$  ( $\text{CO}_2$ -rock) of 1.006 and 1.012 (shown as 'alpha') for siliceous dolomite from Valley (1986). Shifts due to infiltration of a possible magmatic hydrothermal fluid at  $\delta^{13}\text{C}_{(\text{VPDB})} = -5\text{‰}$  and  $\delta^{18}\text{O}_{(\text{VSMOW})} = +6.3\text{‰}$  (Taylor & Sheppard, 1986) at  $T = 300\text{ °C}$  and  $\text{XCO}_2 = 0.1$  and  $0.5$  were modelled using the method of Bowman (1988). The global average for Orosirian calcite marble (star symbol), based on the Precambrian Marine Carbonate Isotope Database of Shields and Veizer (2002), is shown along with the igneous fields for calcite from the mantle (Ray *et al.* 1999) and mantle-derived primary carbonatites (Taylor *et al.* 1967).

6 to 11 ‰ lighter than the isotopic values of average Orosirian carbonate.

In evaluating the causes of the isotopically light C and O isotope values, the following factors need to be considered: 1. The sulphides were likely premetamorphic and subsequently subjected to amphibolite facies regional metamorphism; and 2. Sulphur isotope studies of sulphides suggest the primary involvement of modified seawater in the formation of the deposits, although the contribution of a magmatic-hydrothermal component cannot be discounted. To evaluate the reasons for the isotopically light C and O isotope values, we use the approach taken by Bowman *et al.* (1985) for evaluating the origin of carbonates in hydrothermal systems.

One possible reason for the light isotopic values obtained here is that the marbles spatially associated with sulphide mineralisation may be products of the decarbonation of limestone during the amphibolite facies regional metamorphism. Modelling the effect of decarbonation can be done in two ways (batch volatilisation and Rayleigh volatilisation) that were proposed by Nabelek *et al.* (1984) and Valley (1986). The difference between these two processes is that batch volatilisation involves a closed system with the evolved

fluid equilibrating with the host carbonate, whereas Rayleigh volatilisation involves the continuous exchange and removal of the fluid during the volatilisation process. These processes have been modelled using an  $\alpha$  factor of 1.006 appropriate for the decarbonation of a siliceous dolomite (Valley, 1986) and a higher  $\alpha$  value of 1.012 for comparison purposes, utilising starting  $\delta^{13}\text{C}_{\text{VPDB}}$  and  $\delta^{18}\text{O}_{\text{VSMOW}}$  values of least-altered dolomite (Fig. 7). However, regardless of which  $\alpha$  factor is used, there is a maximum amount of  $^{18}\text{O}$  depletion that occurs via decarbonation reactions (Bowman, 1998). So the effect of decarbonation during the amphibolite facies metamorphism may account for the light values of  $\delta^{13}\text{C}_{\text{VPDB}}$  observed in some Stollberg carbonates but not the isotopic light values of  $\delta^{18}\text{O}_{\text{VSMOW}}$ . Instead, the cause for the shift to light oxygen isotope values is likely a result of heated seawater that was modified as it interacted with the volcanoclastic sequence hosting the sulphide mineralisation. The modified seawater also produced the premetamorphic alteration associated with sulphide formation and an increase in the Mn and Mg content of carbonates that was reported by Jansson *et al.* (2013).

Given the possibility that the unaltered carbonate could have been altered by a magmatic-hydrothermal fluid, the isotopic

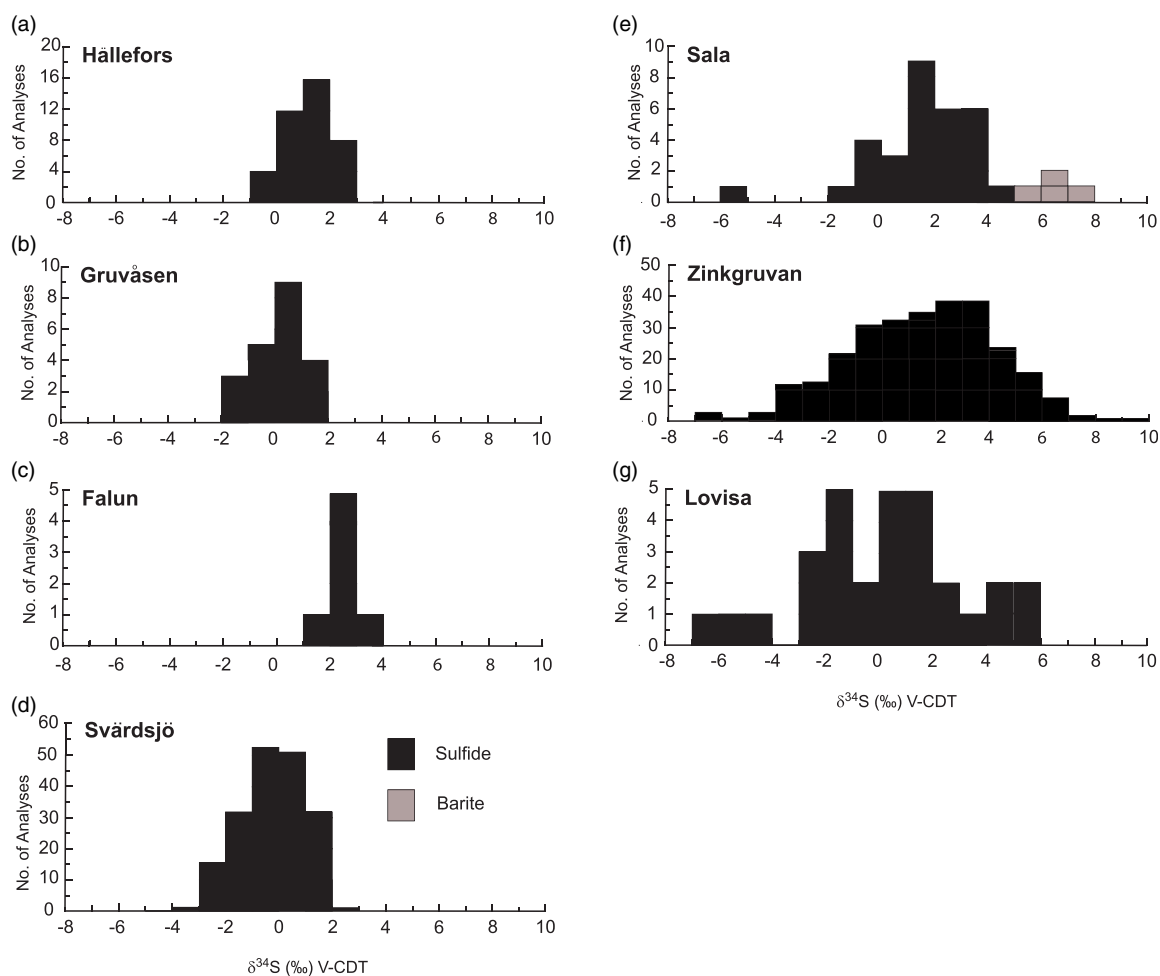


**Figure 8.** Histogram showing sulphur isotope compositions of SVALS- and SAS-type deposits. Data are for the following SVALS-type deposits: (a) Hällefors, Wagner *et al.* (2005); (b) Gruvåsen, Hellingwerf & van Raaphorst (1988); (c) Falun, Gavelin *et al.* (1960); (d) Svärdsjö, Billström *et al.* (1985); and (e) Sala, Jansson *et al.* (2021); and SAS-type deposits (f) Zinkgruvan, Billström (1991) and Jansson *et al.* (2017); (g) Lovisa, Jansson *et al.* (2018).

compositions have also been modelled using a hypothetical fluid of  $\delta^{13}\text{C}_{\text{VPDB}} = -5.0$  ‰ and  $\delta^{18}\text{O}_{\text{VSMOW}} = +6.3$  ‰ (Taylor & Sheppard, 1986) for a  $T = 300$  °C (i.e. midway between the  $T$  range used to calculate the S isotope calculations in Figure 5 and 6) and  $\text{XCO}_2 = 0.1$  and  $0.5$ . The distribution of data obtained here, coupled with those of Billström *et al.* (1985), of light isotope data from Stollberg form an array that is consistent with a magmatic-hydrothermal fluid regardless of the host rock type and location. Note that the shape of the curves will vary only slightly if calculated at  $T = 250$  or  $350$  °C. Although the distribution of the C and O isotope compositions of Stollberg carbonates resembles the knee-shaped curve characteristic of contact skarns where there is an interaction of a limestone horizon with magmatic-hydrothermal fluids from an adjacent causative intrusion, no such intrusive rock is currently known in the Stollberg ore field. The approach taken here has its limitations because it assumes that the knee-shaped trend is due to interaction of a single batch of magmatic-hydrothermal fluid. It ignores the possibility that isotopic compositions were modified during subsequent metamorphism. Another possible explanation for the knee-shaped curve of the isotopic compositions is a hybrid scenario, proposed by Bowman (1998), where early alteration causes a shift to lighter

O isotopic compositions, along with decarbonation of carbonates with different starting C isotopic compositions.

### 6.c. Comparison of stable isotopic compositions with those from other SVALS-, SAS-type deposits in the Bergslagen mining district

Sulphur isotope values of  $\delta^{34}\text{S}_{\text{VCDT}} = +1.12$  to  $+5.71$  ‰ for sulphides at Stollberg with averages of  $+3.15$  to  $+4.46$  ‰ for the three deposits studied here (Fig. 4) are higher than average isotopic composition of sulphides reported to date from other SVALS-type deposits in the Bergslagen district (Hällefors:  $\delta^{34}\text{S}_{\text{VCDT}} = -0.6$  to  $2.7$  ‰, Wagner *et al.* 2003 (Fig. 8a); Gruvåsen:  $-1.4$  to  $+1.5$  ‰, Hellingwerf & van Raaphorst 1988 (Fig. 8b); Falun:  $-2.3$  to  $-0.2$  ‰, Gavelin *et al.* 1960 (Fig. 8c); Svärdsjö:  $-4.0$  to  $+3.0$  ‰, Billström, 1985 (Fig. 8d); and Sala:  $-1.07$  to  $+4.17$  ‰, Jansson *et al.* 2021 (Fig. 8e). Such isotopic values are close to  $0$  ‰ and within the range of  $0 \pm 5$  ‰ generally ascribed to a magmatic-hydrothermal or primordial volcanic source (Ohmoto, 1986). The values near  $0$  ‰ do not discern between a source of sulphur that was derived from a magma or leached from disseminated sulphides in the volcanoclastic pile associated with the deposits. Given that both

sources of sulphur are ultimately the same, it is likely that they have a component of both of these sources. In the Bergslagen district, the dominant sulphide in the volcanic successions is pyrite, so that it is likely that pyrite was dissolved to liberate sulphur, which subsequently reacted with a metal-bearing solution from another source that contained Pb, Zn and Ag.

Although formed from lower temperature fluids (i.e. < 250 °C, Jansson *et al.* 2017, Stephens & Jansson, 2020), the sulphur isotope compositions of sulphides from SAS-type deposits also overlap with those from SVALS-type deposits (i.e. Zinkgruvan:  $\delta^{34}\text{S}_{\text{VCDT}} = -6.5$  to  $+16.5$  ‰ (Fig. 8f), Billström, 1991; Jansson *et al.* 2017; Lovisa:  $-6.1$  to  $+4.7$  ‰ (Fig. 8g), Jansson *et al.* 2018) but generally exhibit a broader isotopic range. Jansson *et al.* (2017) invoked mixing between a magmatic-volcanic sulphur source from spatially related volcanic rocks and a reduced sulphur source derived from graphite-bearing interbedded siltstone, dolomite and mudstone spatially associated with the Zinkgruvan deposit. Stratiform SAS-type mineralisation also characterises the Lovisa Zn-Pb deposit. In this deposit, sulphide-bearing iron formation occurs stratigraphically below banded sphalerite ore, which in turn is overlain by the main ore zone consisting of laminated sphalerite, coarse galena-sphalerite veins and brecciated (durchbewegt) ore. Sulphur isotope compositions vary through the stratigraphic sequence with the isotopically lightest isotope values being associated with impregnated sulphides in the iron formation with the overall isotopically heaviest values in the sphalerite ore. The main ore zone values are centred around 0 ‰ (Jansson *et al.* 2018). The broad range of sulphur isotopic values for sulphides from Lovisa was interpreted by Jansson *et al.* (2018) to be due to mixing of  $\text{H}_2\text{S}$  from TSR and BSR seawater sulphate reduction and sulphur derived from the leaching of volcanic rocks, with the latter source being more important with time as sulphides precipitated in a shallow sedimentary basin.

A knee bend shape distribution of C and O isotopes in carbonates associated with other SVALS-type deposits (i.e. Garpenberg, Saxberget) can be seen in Figure 7 and resembles that shown for carbonates from the Stollberg ore field, although Garpenberg and Saxberget have O isotope values  $\sim +3$  to  $+4$  ‰ lighter than those from the Stollberg ore field. It should be noted that the isotopically lightest C and O isotope compositions for carbonates from the Garpenberg, Saxberget and Stollberg deposits overlap carbonate compositions derived from the mantle and primary carbonatite fields of Ray *et al.* (1999) and Taylor *et al.* (1967), respectively. Although such values support the concept of a magmatic-hydrothermal contribution to the ore fluid, they are not diagnostic of such a contribution. The presence of altered rocks composed of sericite, K-feldspar and pyrite at proposed ore fluid temperatures of around 250 ° to 350 °C and the stabilities of minerals in the system Fe-S-O (assuming that pyrite, pyrrhotite and magnetite are primary) is compatible with a scenario in which the ore fluid was initially acidic and then became more alkaline as it interacted with limestone prior to regional metamorphism. Small reductions in the pH would allow dissolution and replacement of the carbonate by a warm to hot hydrothermal fluid.

Factors, other than the incorporation of a magmatic component to the ore fluid, which may explain the variable light C isotopes in the Bergslagen district include the composition of the ore fluid, the buffering of the wall rock, the nature of structures and lithological contacts, as well as the degree of decarbonation and fluid-rock alteration. For example, light C isotopes can also result from the incorporation of organic matter and hydrocarbons into the ore fluid. Such organic matter occurs in graphitic mudstones spatially

associated with the Zinkgruvan deposit (Jansson *et al.* 2017). In the Bergslagen district, ore-forming fluids which produced a lowering of  $\delta^{18}\text{O}_{\text{VSMOW}}$  also precipitated  $\text{SiO}_2$  into an originally pure dolomite marble. This likely affected subsequent syn-metamorphic decarbonation reactions under amphibolite facies conditions. In such cases, syn-metamorphic decarbonation would more likely occur in an altered marble than in an unaltered marble. Another factor that will possibly affect values of  $\delta^{13}\text{C}_{\text{VPDB}}$  is the control of lithological contacts as well as textural and structural features in the carbonate rocks resulting from premetamorphic alteration (e.g. vugs, breccia etc.) and subsequent syn-metamorphic alteration. For example, dolomitic limestone distal to any synsedimentary fault and away from any lithological contact would be less likely to be significantly altered by hydrothermal fluids, which would result in a lowering of  $\delta^{18}\text{O}_{\text{VSMOW}}$  in comparison with that in limestone proximal to faults. Upon conversion to marble, porosity and permeability would decrease further which would inhibit decarbonation reactions. The isotopic compositions of the carbonates would not follow vectors that trend towards the primary carbonatite/mantle field (i.e. magmatic water box of Sahlström *et al.* 2019) but instead would retain a marine carbonate signature. In contrast, marble close to early faults would probably be more texturally complex and amenable to developing secondary porosity, and reactivated faults would be important in generating permeability to allow the  $\text{CO}_2$  generated by decarbonation reactions to effervesce or be flushed away, which would enhance driving decarbonation reactions. While these scenarios are speculative, they are ways to explain why decarbonation reactions would be more likely to occur in carbonates that were altered or to generate pathways between geological features. Such situations will ultimately produce variability in the C isotope composition among different lithologies and SVALS-/SAS-type deposits in the Bergslagen district.

The results of the current study are in keeping with the tantalising observation made by Billström *et al.* (1985) and Allen *et al.* (2003) that the depletion of  $\delta^{13}\text{C}_{\text{VPDB}}$  (by at least 2 ‰) and  $\delta^{18}\text{O}_{\text{VSMOW}}$  relative to Proterozoic limestone values could potentially be used as an exploration guide to carbonate-related metamorphosed massive sulphide deposits in the Bergslagen district. In the case of  $\delta^{18}\text{O}_{\text{VSMOW}}$  values, Figure 7 suggests that values  $+12$  to  $+15$  ‰ lighter than the isotopic values of average Orosirian carbonate (Shields & Veizer, 2002) are useful indicators of hydrothermal processes, which may be related to, but not necessarily diagnostic of, ore-forming processes.

## Conclusions

Sulphide occurrences in the Stollberg ore field are SVALS-type deposits that formed as semi-massive bodies hosted by marble, skarn and metavolcanic rocks. Modelling of sulphur isotope values, and stabilities in the systems Fe-S-O and K-Al-Si-O-H as well as calcite, for temperatures of 250 ° to 350 °C,  $\delta^{34}\text{S}_{\text{SS}} = +3$  and  $+17$  ‰,  $I = \sim 1$  m NaCl, and a total dissolved S content of  $\sim 0.01$  and 0.1 moles/kg  $\text{H}_2\text{O}$  are most compatible with sulphur being the product of inorganic reduction of Proterozoic seawater sulphate. Sulphur isotope compositions of sulphides from the Stollberg ore field, like those from other SVALS-type deposits, show a narrow range but are slightly heavier than those for other SVALS-type deposits. In comparison, sulphur isotope compositions of sulphides from SAS-type deposits in the Bergslagen district show a wider range of isotopic compositions likely due to the involvement of TSR and BSR of seawater sulphate. Modelling of

carbon and oxygen isotope compositions of calcite from altered rocks and marble in the Stollberg ore field also resemble carbonates from other SVALS-type deposits in that they are isotopically light relative to carbonate in Proterozoic limestones. It is unclear whether marbles in the Stollberg ore field are stromatolitic or not, due to the lack of observed stromatolitic textures. Regardless, the C and O isotope compositions of calcite in the ore field are consistent with the involvement of limestone with modified seawater, which produced oxygen isotopic compositions in calcite lighter than those of spatially related marbles. The same fluids were also responsible for the premetamorphic altered rocks throughout the district. Decarbonation of limestone during the amphibolite facies regional metamorphism resulted in the light C isotope values. We emphasise the role of modified seawater in the ore-forming process since it is compatible with the observed S isotope values of sulphides and the O isotope compositions of carbonates in the Stollberg ore field. However, the incorporation of a magmatic-hydrothermal component to the ore-forming fluid cannot be ruled out. The isotopically light C and O isotope values of carbonates in metamorphosed massive sulphide deposits in the Bergslagen district constitute a potential exploration guide to ores of this type.

**Acknowledgements.** Boliden Mineral AB is gratefully acknowledged for funding this project. Discussions with Magnus Ripa (Geological Survey of Sweden) and Boliden Mineral AB geologists, particularly Hein Raat, Jan Olav-Öst and Eric Lundstam, about the geology of the Stollberg area are very much appreciated. We thank Ed Ripley and Suzanne Ankjersterne for assistance with the sulphur and carbon-oxygen isotope analyses, respectively. Kate Frank assisted with sample collection. The constructive reviews of Iain Pitcairn and an anonymous reviewer are appreciated and improved the quality of the manuscript. Tim Johnson is thanked for his editorial handling of the paper and his comments.

## References

- Allen R, Bull S, Ripa M and Jonsson R (2003) Regional stratigraphy, basin evolution, and the setting of stratabound Zn-Pb-Cu-Ag-Au deposits in Bergslagen, Sweden. Final report for SGU-FoU project 03–1203, 91 pp.
- Allen R, Ripa M and Jansson N (2008) Palaeoproterozoic volcanic- and limestone-hosted Zn-Pb-Ag-(Cu-Au) massive sulphide deposits and Fe oxide deposits in Bergslagen, Sweden. International Geological Correlation Program Project 502, Global Comparison of Volcanic-hosted Massive Sulphide Deposits, 33rd International Geological Congress Excursion No. 12, 84 p.
- Allen RL, Lundström I, Ripa M, Simeonov A and Christofferson H (1996) Facies analysis of a 1.9 Ga, continental margin, back-arc, felsic caldera province with diverse Zn-Pb-Ag-(Cu-Au) sulfide and Fe oxide deposits, Bergslagen region, Sweden. *Economic Geology* **91**, 979–1008.
- Andersson UB, Larsson L and Wikström A (1992) Charnockites, pyroxene granulites and garnet-cordierite gneisses at a boundary between Early Svecofennian rocks and Småland-Värmland granitoids, Karlskoga, southern Sweden. *Geologiska Föreningens i Stockholm Förhandlingar* **114**, 1–15.
- Beetsma JJ (1992) Retrograde fluid evolution of the Stollberg Pb-Zn-Fe-Mn (Ag) ore deposit, central Bergslagen, Sweden. *Geologiska Föreningens i Stockholm Förhandlingar* **114**, 279–300.
- Beunk FF and Kuipers G (2012) The Bergslagen ore province, Sweden: review and update of an accreted orocline, 1.9–1.8 Ga BP. *Precambrian Research* **216–219**, 95–119.
- Billström K (1985) *Isotopic studies of two early Proterozoic sulphide ores in the Bergslagen district, south-central Sweden*. Ph.D. thesis, Stockholm University, Sweden, 69 pp.
- Billström K (1991) Sulphur isotope compositions in the Åmmeberg Zn-Pb ore deposit, south-central Sweden: genetic implications. *Geologische Rundschau* **80**, 717–27.
- Billström K, Åberg G and Nord A (1985) Stable isotope data of Bergslagen carbonates and their potential use for sulphide ore prospecting. *Geologiska Föreningens i Stockholm Förhandlingar* **107**, 169–73.
- Björklund E (2011) *Mineralogy and lithogeochemical signature of a stratigraphic profile through the Grängsgruvan Zn-mineralization, Bergslagen, Sweden*. M.S. thesis, Uppsala University, Sweden, 56 pp.
- Bowman JR (1998) Stable-isotope systematics of skarns. In *Mineralized intrusion-related skarn systems* (ed. DR Lentz), pp. 99–145. Mineralogical Association of Canada Short Course Series 26.
- Bowman JR, O'Neil JR and Essene EJ (1985) Contact skarn formation at Elkhorn, Montana. *American Journal of Science* **285**, 621–60.
- Claypool GE, Holser WT, Kaplan IR, Sakai H and Zak I (1980) The age curves of sulfur and oxygen isotopes in marine sulfate and their mutual interpretation. *Chemical Geology* **28**, 199–260.
- De Groot PA and Sheppard SMF (1988) Carbonate rocks from W. Bergslagen, central Sweden: isotopic (C, O, H) evidence for marine deposition and alteration by hydrothermal processes. *Geologie en Mijnbouw* **67**, 177–88.
- Fahlvik A, Kampmann TC and Jansson NF (2022) Hydrothermal alteration, lithogeochemical marker units and vectors towards mineralisation at the Svärdsjö Zn-Pb-Cu deposit, Bergslagen, Sweden. *GFF* **144**, 177–95. <https://doi.org/10.1080/11035897.2022.2120065>.
- Frank KS, Spry PG, Raat H, Allen RL, Jansson NF and Ripa M (2019) Variability in the geological, mineralogical, and geochemical characteristics of base metal sulfide deposits in the Stollberg ore field, Bergslagen, Sweden. *Economic Geology* **114**, 473–52.
- Frank KS, Spry PG, O'Brien JJ, Koenig A, Allen RL and Jansson NF (2022) Magnetite as a provenance and exploration tool to metamorphosed base metal sulfide deposits in the Stollberg ore field, Bergslagen, Sweden. *Mineralogical Magazine* **86**, 373–96.
- Gavelin S, Parwel A and Ryhage R (1960) Sulfur isotope fractionation in sulfide mineralization. *Economic Geology* **55**, 510–30.
- Gebeyehu M and Vivallo W (1991) Sulfide ore genesis and related dolomitization of limestone in the Garpenberg district, south central Sweden: Geochemical and C-O isotope evidence. In *Source, Transport and Deposition of Metals* (eds M Pagel and JL Leroy), pp. 281–83. AA Balkema, Rotterdam.
- Gilligan LB and Marshall B (1987) Textural evidence for remobilization in metamorphic environments. *Ore Geology Reviews* **2**, 205–30.
- Hedström P, Simeonov A and Malmström L (1989) The Zinkgruvan ore deposit, south-central Sweden: A Proterozoic, proximal Zn-Pb-Ag deposit in distal volcanic facies. *Economic Geology* **84**, 1235–61.
- Hellingwerf RH and van Raaphorst JG (1988) Sulphur isotopes from the Gruvåsen sulphide skarn deposit, Bergslagen, Sweden. *Mineralogy and Petrology* **38**, 161–70.
- Hemley JJ (1959) Some mineralogical equilibria in the system  $K_2O-Al_2O_3-SiO_2-H_2O$ . *American Journal of Science* **257**, 241–70.
- Jansson N and Allen R (2020) Using iron formations during exploration for c. 1.9 Ga Zn-Pb-Ag sulphide deposits, Jugansbo area, Bergslagen, Sweden. *EGU General Assembly 2020, Online, 4–8 May 2020, EGU2020-8482*, <https://doi.org/10.5194/egusphere-egu2020-8482>.
- Jansson NF (2017) Structural evolution of the Paleoproterozoic Sala stratabound Zn-Pb-Ag carbonate-replacement deposit, Bergslagen, Sweden. *GFF* **139**, 21–35.
- Jansson NF, Erismann F, Lundstam E and Allen RL (2013) Evolution of the Paleoproterozoic volcanic-limestone-hydrothermal sediment succession and Zn-Pb-Ag and Fe-oxide deposits at Stollberg, Bergslagen, Sweden. *Economic Geology* **108**, 309–35.
- Jansson NF, Zetterqvist A, Malmström L and Allen RL (2017) Genesis of the Zinkgruvan stratiform Zn-Pb-Ag deposit and associated dolomite-hosted Cu ore, Bergslagen, Sweden. *Ore Geology Reviews* **82**, 285–308.
- Jansson NF, Sädbom S, Allen RL, Billström K and Spry PG (2018) The Lovisa stratiform Zn-Pb deposit, Bergslagen, Sweden – Structure, stratigraphy and ore genesis. *Economic Geology* **113**, 699–739.
- Jansson NF, Allen RL, Skogsmo G and Turner T (2021) Origin of Paleoproterozoic, sub-seafloor Zn-Pb-Ag skarn deposits, Sala area, Bergslagen, Sweden. *Mineralium Deposita* **57**, 455–80.
- Jonsson E and Boyce AJ (2002) Carbon and oxygen isotopes as indicators of hydrothermal processes in the Långban area, Bergslagen. *GFF* **124**, 234–5.

- Kampmann TC, Jansson NF, Stephens MB, Majka J and Lasskogen J** (2017) Systematics of hydrothermal alteration at the Falun base metal sulfide deposit and implications for ore genesis and exploration, Bergslagen ore district, Fennoscandian Shield, Sweden. *Economic Geology* **112**, 1111–52.
- Månsson S** (1979) Preliminär rapport. *Geologiska undersökningar, Stollbergsfältet*, **103**, 8.
- McCrea JM** (1950) On the isotopic composition of carbonates and a paleotemperature scale. *Journal of Chemical Physics* **18**, 849–57.
- Nabelek PI, Labotka TC, O'Neil JR and Papike JJ** (1984) Contrasting fluid/rock interaction between the Notch Peak granitic intrusion and argillites and limestone in western Utah: evidence from stable isotopes and phase assemblages. *Contributions to Mineralogy and Petrology* **86**, 25–34.
- Ohmoto H** (1972) Systematics of sulfur and carbon isotopes in hydrothermal ore deposits. *Economic Geology* **67**, 557–78.
- Ohmoto H** (1986) Stable isotope geochemistry of ore deposits. *Reviews in Mineralogy* **16**, 491–559.
- Raat H, Jansson NF and Lundstam E** (2013) The Gränsgruvan Zn-Pb-Ag deposit, an outsider in the Stollberg ore field, Bergslagen, Sweden. In *Mineral deposit research for a high-tech world* (eds E Jonsson, E et al.), Proceedings of the 12th Biennial Geology Applied to Mineral Deposits Meeting, 12–15 August, 2013, Volume 4, Uppsala, Sweden.
- Ray JS, Ramesh R and Pande K** (1999) Carbon isotopes in Kerguelen plume-derived carbonatites: evidence for recycled inorganic carbon. *Earth and Planetary Science Letters* **170**, 205–14.
- Ripa M** (1988) Geochemistry of wall-rock alteration and of mixed volcanic-exhalative facies at the Proterozoic Stollberg Fe-Pb-Zn-Mn(-Ag)-deposit, Bergslagen, Sweden. *Geologie en Mijnbouw* **67**, 443–57.
- Ripa M** (1994) The mineral chemistry of hydrothermally altered and metamorphosed wall-rocks at the Stollberg Fe-Pb-Zn-Mn(-Ag) deposit, Bergslagen, Sweden. *Mineralium Deposita* **29**, 180–8.
- Ripa M** (1996) *The Stollberg ore field – petrography, litho-geochemistry, mineral chemistry, and ore formation*. Ph.D. thesis, Lund University, Sweden, 23 pp.
- Ripa M** (2012) Metal zonation in alteration assemblages at the volcanogenic Stollberg Fe-Pb-Zn-Mn(-Ag) skarn deposit, Bergslagen, Sweden. *GFF* **134**, 317–30.
- Ripa M, Sundberg A, Wik N-G, Bergman T, Claeson D, Hallberg A, Hellström F, Kübler L and Nysten P** (2015) Malmer, industriella mineral och bergarter i Dalarnas län. *Sveriges geologiska undersökning* **139**, 316.
- Sahlström F, Jonsson E, Högdahl K, Troll VR, Harris C, Jolis EM and Weis F** (2019) Interaction between high-temperature magmatic fluids and limestone explains 'Bastnäs-type' REE deposits in central Sweden. *Nature Scientific Reports* **9**, 15203.
- Schildes G and Veizer J** (2002) Precambrian marine carbonate isotope database: Version 1.1. *Geochemistry, Geophysics, Geosystems* **3**, 12. <http://g-cubed.org/gc2002/2001GC000266>.
- Selinus O** (1983) Factor and discriminant analysis to litho-geochemical prospecting in an area of central Sweden. *Journal of Geochemical Exploration* **19**, 619–42.
- Stephens MB and Bergman S** (2020) Regional context and lithotectonic framework of the 2.0–1.8 Ga Svecokarelian orogeny, eastern Sweden. *Geological Society London, Memoirs* **50**, 19–26.
- Stephens MB and Jansson NF** (2020) Paleoproterozoic (1.9–1.8 Ga) synorogenic magmatism, sedimentation and mineralization in the Bergslagen lithotectonic unit, Svecokarelian orogen. *Geological Society London, Memoirs* **50**, 155–206.
- Stephens MB, Ripa M, Lundström I, Persson L, Bergman T, Ahl M, Wahlgren C-H, Persson PH and Wickström L** (2009) Synthesis of the bedrock geology in the Bergslagen region, Fennoscandian Shield, south-central Sweden. *Sveriges geologiska undersökning* **Ba58**, 259.
- Studley SA, Ripley EM, Elswick ER, Dorais MJ, Fong J, Finkelstein D and Pratt LM** (2002) Analysis of sulfides in whole rock matrices by elemental analyzer-continuous flow isotope ratio mass spectrometry. *Chemical Geology* **192**, 141–8.
- Taylor HP Jr, Frechen J and Degens ET** (1967) Oxygen and carbon isotope studies of carbonatites from the Laacher See district, West Germany and the Alnö District, Sweden. *Geochimica et Cosmochimica Acta* **31**, 407–30.
- Taylor HP Jr and Sheppard SMF** (1986) Igneous rocks: I. Process of isotopic fractionation and isotope systematics. *Reviews in Mineralogy* **16**, 445–89.
- Valley J** (1986) Stable isotope geochemistry of metamorphic rocks. *Reviews in Mineralogy* **16**, 445–89.
- Wagner T, Jonsson E and Boyce AJ** (2005) Metamorphic ore remobilization in the Hällefors district, Bergslagen, Sweden: constraints from mineralogical and small-scale sulphur isotope studies. *Mineralium Deposita* **40**, 100–14.
- Warr L** (2021) IMA-CNMNC approved mineral symbols. *Mineralogical Magazine* **85**, 291–320.
- Weihed P, Arndt N, Billström K, Duchesne J-C, Eilu P, Martinsson O, Papunen H and Lahtinen R** (2005) 8: Precambrian geodynamics and ore formation: The Fennoscandian Shield. *Ore Geology Reviews* **17**, 273–322.